Transmembrane Protein Aptamer Induces Cooperative Signaling by the EPO Receptor and the Cytokine Receptor -Common Subunit

He, Li; Cohen, Emily B.; Edwards, Anne P. B.; Xavier-Ferrucio, Juliana; Bugge, Katrine; Federman, Ross S.; Absher, Devin; Myers, Richard M.; Kragelund, Birthe B.; Krause, Diane S.; DiMaio, Daniel

Published in:
iScience

DOI:
10.1016/j.isci.2019.06.027

Publication date:
2019

Document version
Publisher's PDF, also known as Version of record

iScience

CellPress

Article

Transmembrane Protein Aptamer Induces Cooperative Signaling by the EPO Receptor and the Cytokine Receptor β-Common Subunit

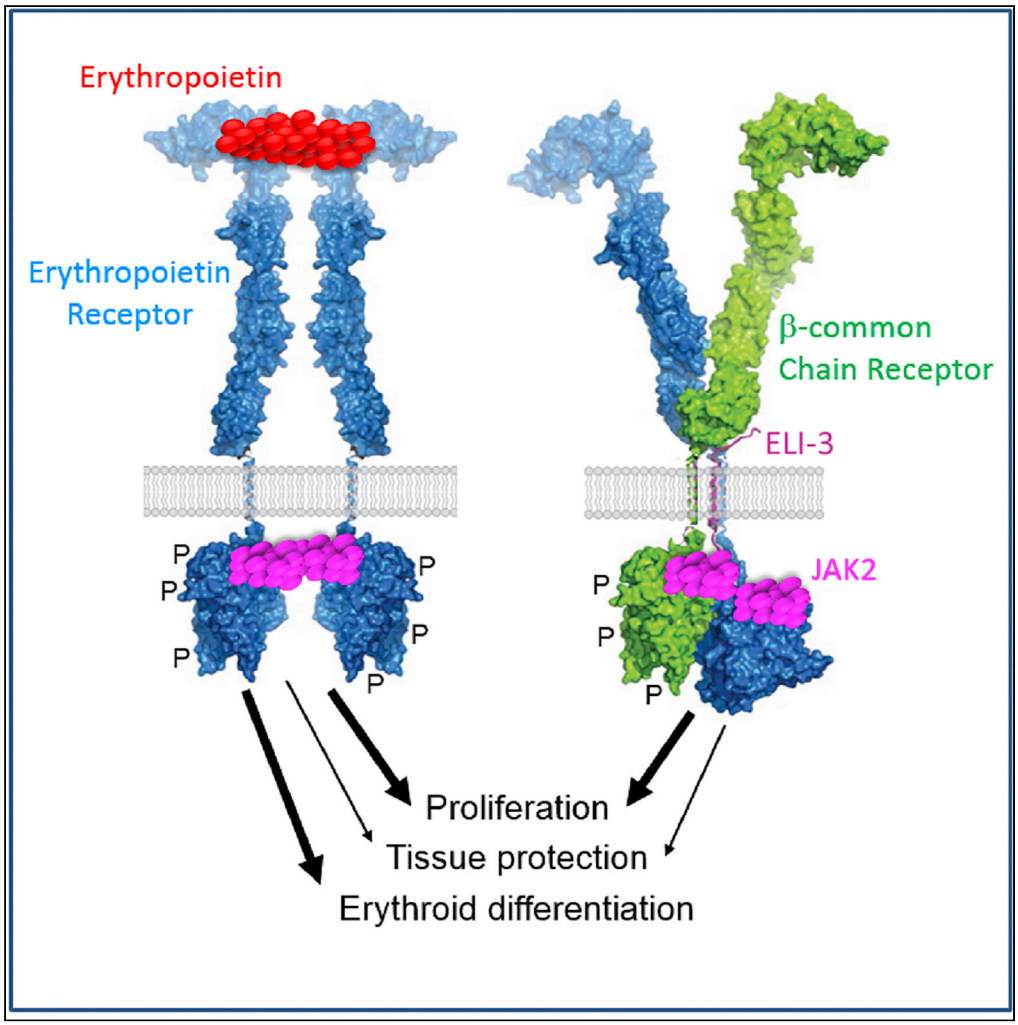

Li He, Emily B. Cohen, Anne P.B. Edwards, ..., Birthe B. Kragelund, Diane S. Krause, Daniel DiMaio

daniel.dimaio@yale.edu

HIGHLIGHTS

46-residue artificial transmembrane protein can activate the erythropoietin receptor

Activation of the EPOR also requires the cytokine receptor β-common chain

Activation does not require the EPOR cytoplasmic tyrosines

Active heteroreceptor supports cell proliferation but not erythroid differentiation

He et al., iScience *17*, 167–181
July 26, 2019
https://doi.org/10.1016/j.isci.2019.06.027

iScience

CellPress

Article

Transmembrane Protein Aptamer Induces Cooperative Signaling by the EPO Receptor and the Cytokine Receptor β-Common Subunit

Li He,[1] Emily B. Cohen,[1,9] Anne P.B. Edwards,[1] Juliana Xavier-Ferrucio,[2] Katrine Bugge,[3] Ross S. Federman,[4] Devin Absher,[5] Richard M. Myers,[5] Birthe B. Kragelund,[3] Diane S. Krause,[2,8] and Daniel DiMaio[1,6,7,8,10,*]

SUMMARY

The erythropoietin receptor (EPOR) plays an essential role in erythropoiesis and other cellular processes by forming distinct signaling complexes composed of EPOR homodimers or hetero-oligomers between the EPOR and another receptor, but the mechanism of heteroreceptor assembly and signaling is poorly understood. We report here a 46-residue, artificial transmembrane protein aptamer, designated ELI-3, that binds and activates the EPOR and induces growth factor independence in murine BaF3 cells expressing the EPOR. ELI-3 requires the transmembrane domain and JAK2-binding sites of the EPOR for activity, but not the cytoplasmic tyrosines that mediate canonical EPOR signaling. Instead, ELI-3-induced proliferation and activation of JAK/STAT signaling requires the transmembrane and cytoplasmic domains of the cytokine receptor β-common subunit (βcR) in addition to the EPOR. Moreover, ELI-3 fails to induce erythroid differentiation of primary human hematopoietic progenitor cells but inhibits nonhematopoietic cell death induced by serum withdrawal.

INTRODUCTION

Many aspects of cell behavior are controlled by cell surface receptors that receive extracellular signals and orchestrate the cellular response. The formation and activation of alternative receptor complexes with different subunits and signaling properties can dictate receptor output (e.g., Kovacs et al., 2015). The cytokine erythropoietin (EPO) can activate alternative complexes of the EPO receptor (EPOR), a transmembrane (TM) cell surface protein lacking intrinsic kinase activity. Binding of EPO to the EPOR can trigger the homodimerization of EPORs in a productive orientation, leading to the transphosphorylation of Janus kinase 2 (JAK2), which is constitutively associated with the EPOR (Constantinescu et al., 1999a, 2001; Watowich et al., 1999). Activated JAK2 phosphorylates multiple tyrosines in the intracellular domain of EPOR, allowing the recruitment and phosphorylation of downstream signaling proteins, including signal transducer and activator of transcription 5 (STAT5) (Barber et al., 1997; Kuhrt and Wojchowski, 2015; Sawyer and Penta, 1996; Lodish et al., 2009). This signaling pathway is essential for the survival, proliferation, and differentiation of erythroid progenitors.

In addition to erythropoiesis, the EPOR can mediate non-erythroid outcomes in response to EPO treatment, including a tissue-protective response that prevents apoptosis and promotes proliferation in non-hematopoietic cells subjected to injury or metabolic stress (Acharya et al., 2010; Brines, 2010; Jubinsky et al., 1997; Siren and Ehrenreich, 2001; Siren et al., 2001a, 2001b; Jelkmann et al., 2009), reviewed in Jelkmann et al. (2009). The protective effect of EPO appears to require the activation of a heteroreceptor composed of EPOR and the cytokine receptor β-common subunit (β-common receptor [βcR] also known as CD131). In addition to constitutively binding EPOR, βcR also binds the α-chain of interleukin (IL)-3 receptor, granulocyte-macrophage colony-stimulating factor (GM-CSF) receptor (GM-CSFR), and IL-5 receptor (Blake et al., 2002; Jubinsky et al., 1997; Hercus et al., 2013; Lopez et al., 1992). βcR plays an essential role in signaling by these receptors, which lack JAK2 binding or a significant cytoplasmic domain, by providing bound JAK2 and cytoplasmic tyrosines for phosphorylation (Hansen et al., 2008; Hercus et al., 2013). $\beta cR^{-/-}$ mice lack EPO-induced tissue protection but retain normal hematopoiesis, showing that βcR is required for tissue protection but not for erythroid differentiation in at least some settings (Weber et al., 2005; Brines et al., 2004). In addition, certain modified versions of EPO, such as lysine-carbamylated EPO, specifically induce the tissue-protective, but not the erythroid, effects of EPO (Erbayraktar et al., 2009; Leist et al., 2004; Murphy and Young, 2006; Yamanaka et al., 2018). These results suggest that the tissue-protective

[1]Department of Genetics, Yale School of Medicine, P.O. Box 208005, New Haven, CT 06520-8005, USA

[2]Department of Laboratory Medicine, Yale School of Medicine, P.O. Box 208073, New Haven, CT 06520-8073, USA

[3]Structural Biology and NMR Laboratory, The Linderstrøm-Lang Centre for Protein Science and Integrative Structural Biology at University of Copenhagen (ISBUC), Department of Biology, University of Copenhagen, Copenhagen N 2200, Denmark

[4]Department of Immunobiology, Yale School of Medicine, P.O. Box 208011, New Haven, CT 06520-8011, USA

[5]HudsonAlpha Institute for Biotechnology, 601 Genome Way, Huntsville, AL 35806, USA

[6]Department of Therapeutic Radiology, Yale School of Medicine, P.O. Box 208040, New Haven, CT 06520-8040, USA

[7]Department of Molecular Biophysics & Biochemistry, P.O. Box 208114, Yale University, New Haven, CT 06520-8114, USA

[8]Yale Cancer Center, P.O. Box 208028, New Haven, CT 06520-8028, USA

[9]Present address: Beth Israel Deaconess Medical Center, Harvard Medical School, Boston, MA 02215, USA

[10]Lead Contact

*Correspondence: daniel.dimaio@yale.edu

https://doi.org/10.1016/j.isci.2019.06.027

effect of EPO is mediated by an EPOR/βcR heteroreceptor, and not by EPOR homodimerization (Bohr et al., 2015). However, the role of the heteroreceptor in tissue protection remains controversial (see citations in Cheung Tung Shing et al. 2018), and in some situations a classical EPOR homodimer can provide a protective signal (Um et al., 2007). Notably, the elements on the EPOR and βcR required for heteroreceptor formation and the molecular mechanism of signaling by the βcR/EPOR heteroreceptor are unknown.

Various receptors, including the EPOR, can be activated through interactions involving their TM domain (TMD). The murine spleen focus-forming virus envelope protein gp55-P specifically binds to the TMD of the mouse EPOR (mEPOR), triggering EPOR activation, erythroid cell proliferation, and polycythemia (Li et al., 1990; Constantinescu et al., 1999b). The platelet-derived growth factor β receptor (PDGFβR) can be activated by the bovine papillomavirus E5 oncoprotein, a 44-residue TM protein that binds specifically to the TMD of the PDGFβR (DiMaio and Petti, 2013; Petti and DiMaio, 1992; Petti et al., 1991). We developed a genetic approach to isolate small biologically active TM proteins in which we construct libraries expressing up to millions of different, small, artificial TM proteins (termed *traptamers*, for TM aptamers) with randomized, hydrophobic segments. Traptamer libraries are expressed in mammalian cells, and active traptamers are recovered from cells selected for particular biological activities, with the rationale that, by chance, rare traptamers interact with cellular TM proteins and modulate their activity or expression (Cammett et al., 2010; Freeman-Cook et al., 2004; Freeman-Cook and DiMaio, 2005; Scheideman et al., 2012). We have isolated traptamers that specifically activate human EPOR (hEPOR) or mEPOR and cause EPOR-dependent proliferation of murine BaF3 cells (Cammett et al., 2010; Cohen et al., 2014; He et al., 2017). These traptamers bind the TMD of the EPOR and induce hEPOR homodimerization and tyrosine phosphorylation of EPOR and JAK2.

Here, we isolate and characterize a new traptamer, ELI-3, that induces proliferation of BaF3 cells that express the EPOR. ELI-3 interacts with the hEPOR and, unlike EPO or previously isolated traptamers that activate the EPOR, does not require intracellular hEPOR tyrosines, but instead requires the endogenously expressed βcR in addition to the EPOR. ELI-3 does not support differentiation in erythroid cells and inhibits serum withdrawal-induced apoptosis in non-hematopoietic cells. These results show that small TM proteins can specifically activate either the EPOR homodimer or the EPOR/βcR heteroreceptor, with distinct biological outcomes. Our results also demonstrate that the EPOR in the EPOR/βcR heteroreceptor uses a non-canonical mechanism to generate a proliferative signal.

RESULTS

Isolation of a Traptamer that Confers Growth Factor Independence in Cells Expressing hEPOR

The strategy used to isolate new traptamers that cooperate with the EPOR is shown in Figure 1A. We used the YX4 traptamer expression library, in which the TMD of the bovine papillomavirus E5 protein is replaced with a 24-residue stretch of randomized, primarily hydrophobic amino acids (Figure 1B) (Scheideman et al., 2012). The traptamers also contain an N-terminal hemagglutinin (HA) epitope tag. The YX4 library was packaged into retrovirus and used to infect BaF3 cells expressing the hEPOR (BaF3/hEPOR cells) at a low MOI so that most cells received a single infectious retrovirus particle. As a control, cells were infected with empty retrovirus vector, MSCVpuro. BaF3/hEPOR cells normally require IL-3 for proliferation, but EPO or proteins that activate the hEPOR can replace EPO. After puromycin selection, transduced cells were incubated in medium lacking growth factors. As expected, cells expressing MSCVpuro died, but cultures infected with the YX4 library proliferated. After 8 days in medium lacking growth factors, genomic DNA was extracted from proliferating cells and the retroviral inserts were amplified and subjected to next-generation sequencing, which produced over 4 million proper read pairs consistent with the design of the library. We focused on the 278 most abundant sequences. Sequences that lacked frameshift mutations were sorted into 105 groups based on sequence similarity. The frequency of sequences in each group ranged from 0.01% to 6.99%. Sequencing of the starting library plasmid DNA showed no abundant sequences.

We expressed seven of the most abundant selected sequences (Figure 1C) in parental BaF3 cells and in BaF3/hEPOR cells. Most of these constructs conferred growth factor independence in both cell lines (Figure 1D), suggesting that they acted through a protein expressed in parental cells. In contrast, the 46-residue ELI-3 traptamer conferred growth factor independence in BaF3/hEPOR cells, but not in parental BaF3 cells, demonstrating that ELI-3 required the hEPOR for activity.

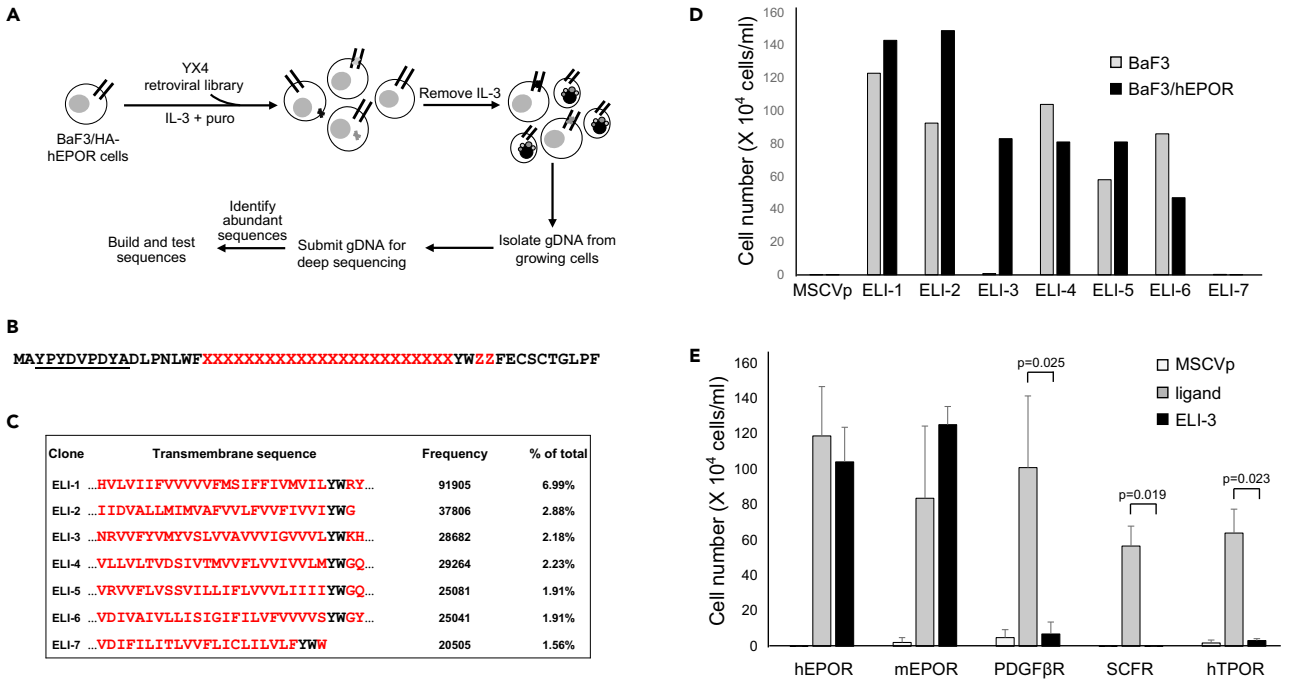

Figure 1. Isolation of a New Traptamer that Cooperates with the EPOR to Confer Growth Factor Independence

(A) Scheme to isolate traptamers that cooperate with the hEPOR. BaF3/hEPOR cells were infected with retroviruses expressing the YX4 traptamer library, selected with puromycin, and then incubated in medium lacking growth factors. Genes encoding traptamers were recovered from genomic DNA isolated from live cells after selection and then subjected to deep sequencing. Abundant sequences were synthesized and tested for activity. Black bars represent exogenous hEPOR; black and gray "X"s represent traptamers.

(B) The design of the YX4 library is shown in the single-letter amino acid representation. Randomized residues are colored red. The X's represent randomized positions, each with an 80% probability of encoding a hydrophobic amino acid. The Z's represent randomized amino acids with an ~30% chance of being a stop codon. The N-terminal HA tag is underlined.

(C) Abundant sequences recovered from growth factor-independent BaF3/hEPOR cells. The randomized regions are colored red. The invariant YW are colored black. The frequency of the sequence (and closely related sequences) and its proportion among all sequences obtained are listed.

(D) BaF3 and BaF3/hEPOR cells stably expressing empty vector (MSCVp) or a traptamer listed in (C) were incubated in medium lacking IL-3. The number of live cells 4 days after IL-3 removal is shown for a representative experiment.

(E) BaF3 cells expressing hEPOR, mEPOR, PDGFβR, stem cell factor receptor (SCFR), or human thrombopoietin receptor (hTPOR) were infected with MSCVp or MSCVp expressing ELI-3. After puromycin selection, cells were incubated in medium lacking IL-3. Where indicated, cells expressing MSCVp were also incubated in medium containing the cognate ligand: EPO for hEPOR and mEPOR, PDGF-BB for PDGFβR, stem cell factor for SCFR, and TPO for hTPOR. The number of live cells 4 days after IL-3 removal is shown. The averaged results and standard deviation of three independent experiments are shown. Statistical significance was evaluated by two-tailed Student's t test with unequal variance.

To examine the specificity of ELI-3, we introduced it into BaF3 cells expressing hEPOR, mEPOR, the human thrombopoietin receptor, PDGFβR, or stem cell factor receptor. After IL-3 removal, cells expressing each receptor proliferated in response to its ligand, but not in the absence of ligand (Figure 1E). Notably, ELI-3 induced IL-3 independence only in cells expressing hEPOR or mEPOR (Figure 1E), indicating that ELI-3 activity was specific to EPOR and that it cooperated with either hEPOR or mEPOR, whose TMDs differ at only three residues and adopt a similar α-helical structure (Li et al., 2015).

ELI-3 Forms a Stable Complex with the hEPOR and Requires Specific Residues in the EPOR Transmembrane Domain

We used co-immunoprecipitation to determine if ELI-3 and hEPOR were present in a stable complex. First, the HA epitope tag at the N terminus of ELI-3 was replaced with a FLAG epitope tag to generate F-ELI-3. The FLAG tag did not affect the ability of ELI-3 to induce IL-3 independence in BaF3/hEPOR cells (Figure S1). Detergent extracts were prepared from BaF3/hEPOR cells expressing either MSCVpuro or F-ELI-3 and immunoprecipitated with anti-FLAG antibody. After gel electrophoresis and transfer, membranes were immunoblotted with an anti-HA antibody, which recognizes HA-tagged hEPOR. As shown

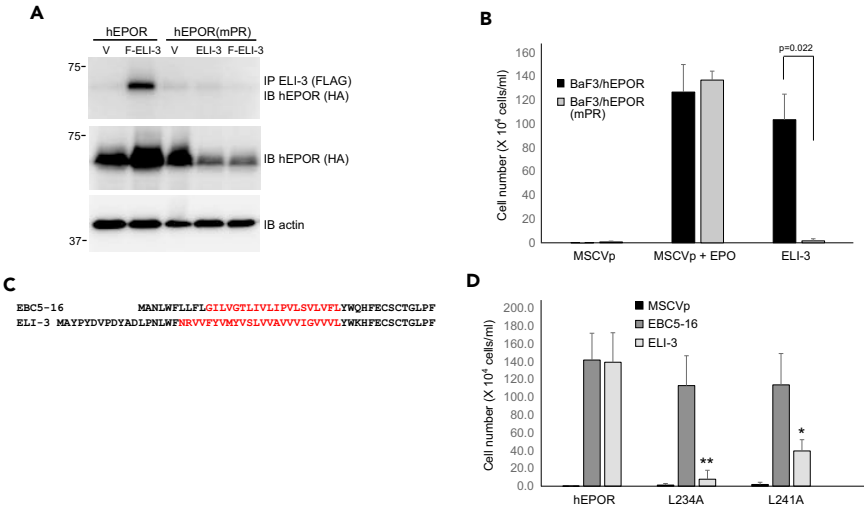

Figure 2. ELI-3 Interacts with the Transmembrane Domain of hEPOR

(A) Extracts prepared from BaF3/hEPOR and BaF3/hEPOR(mPR) cells growing in IL-3 expressing MSCVp (V), ELI-3, or FLAG-tagged ELI-3 (F-ELI-3) were subjected to gel electrophoresis either directly (middle and bottom panels) or after immunoprecipitation with anti-FLAG agarose beads (top panel). After transfer, membranes were immunoblotted with anti-HA antibody to detect EPOR or anti-pan-actin antibody as a loading control.

(B) BaF3/hEPOR and BaF3/hEPOR(mPR) cells stably expressing MSCVp or ELI-3 were incubated in medium lacking IL-3. Where indicated, cells expressing MSCVp were incubated in medium containing EPO. The number of live cells 4 days after IL-3 removal is shown. The averaged results and standard deviation of three independent experiments are shown. Statistical significance was evaluated by two-tailed Student's t test with unequal variance.

(C) The sequences of EBC5-16 and ELI-3. Randomized hydrophobic segments are shown in red.

(D) BaF3 cells expressing the wild-type hEPOR, hEPOR mutant L234A, or mutant L241A were infected with retroviruses to express MSCVp, EBC5-16, or ELI-3. After puromycin selection, cells were incubated in medium lacking IL-3. The number of live cells 4 days after IL-3 removal is shown. The averaged results and standard deviation of three independent experiments are shown. Statistical significance was evaluated by two-tailed Student's t test with unequal variance, comparing cell number in cells expressing wild-type receptor to cell number in cells with mutant receptor expressing the same traptamer. *$p < 0.05$, **$p < 0.01$.

See also Figure S1.

in Figure 2A, anti-FLAG co-immunoprecipitated the hEPOR from cells expressing F-ELI-3, but not from cells expressing MSCVpuro, demonstrating that F-ELI-3 and the hEPOR co-existed in a physical complex.

To determine whether the TMD of hEPOR is required for ELI-3 function, a chimeric hEPOR was used in which the TMD of hEPOR was replaced with the TMD of mouse PDGFβR (designated hEPOR(mPR)). BaF3/hEPOR(mPR) cells were able to grow when IL-3 in the medium was replaced with EPO, demonstrating that hEPOR(mPR) was functional (Figure 2B). However, ELI-3 did not confer growth factor independence on BaF3/hEPOR(mPR) cells (Figure 2B), and F-ELI-3 did not co-immunoprecipitate with hEPOR(mPR) (Figure 2A), showing that the TMD of hEPOR was critical for ELI-3 activity and complex formation between ELI-3 and EPOR.

We next identified hEPOR TMD residues required for the activity of ELI-3 and the previously described traptamer EBC5-16, which activates hEPOR but not mEPOR (Cohen et al., 2014). The TMD sequences of EBC5-16 and ELI-3 are entirely different (Figure 2C). We tested two hEPOR TMD mutants, L234A and L241A. As expected, these receptor mutants did not confer IL-3 independence in BaF3 cells lacking traptamer expression but allowed the cells to proliferate in response to EPO (data not shown). EBC5-16 cooperated well with both EPOR mutants to confer growth-factor independence, whereas ELI-3 failed to cooperate with L234A and displayed markedly reduced activity with L241A (Figure 2D). These results showed that the traptamers required different amino acids in hEPOR TMD, suggesting that the two traptamers interact with the TMD of the hEPOR in distinct manners.

The experiments described above imply that ELI-3 recognizes the TMD of the hEPOR. We conducted biophysical experiments to explore this possibility in more detail. We expressed recombinant ELI-3 in bacteria,

purified it, and subjected it to circular dichroism analysis in detergent micelles. As shown in Figure S2, ELI-3 displayed minima at 208 and 222 nm, characteristic of α-helical structure, as expected. We then mixed ELI-3 with purified ^{15}N-labeled TMD plus flanking sequences of the hEPOR (residues 217–252) and conducted solution NMR spectroscopy in the presence of different concentrations of the detergent, 1,2-dihexanoyl-sn-glycero-3-phosphocholine (DHPC) (Figure S3, red peaks). For comparison, the same analysis was also performed for ^{15}N-labeled hEPOR$_{217\text{-}252}$ in the absence of ELI-3 (Figure S3, black peaks). The addition of ELI-3 caused a detergent-sensitive perturbation of the majority of the hEPOR-TMD chemical shifts toward the dimeric state (Figures S3A and S3B). This suggests that the presence of ELI-3 stabilizes a dimeric state of the hEPOR-TMD, as we showed previously with other hEPOR-specific traptamers (He et al., 2017). This effect likely occurs through direct interactions between these two proteins, because detergent alone could not populate the dimer to the same extent as did ELI-3. Because of the inherent challenges in using NMR spectroscopy to study the interaction of these hydrophobic peptides, we focused our further efforts on analyzing ELI-3 activity in cells.

ELI-3 Does Not Induce Erythroid Differentiation

We previously showed that EBC5-16 supported erythroid differentiation of CD34$^+$ human hematopoietic progenitor cells (hHPCs) *in vitro* in the absence of EPO (Cohen et al., 2014). Here, we used a more quantitative assay to assess whether EBC5-16 or ELI-3 promoted erythroid differentiation in primary human megakaryocyte-erythroid progenitor (MEP) cells, which give rise to colonies containing erythroid or megakaryocytic cells (or both) when cultured *in vitro* with a cocktail of cytokines including EPO. MEP cells isolated on the basis of expression of cell surface markers (see Methods, Sanada et al., 2016) were infected with MSCVpuro or with retroviruses expressing EBC5-16 or ELI-3. Transduced cells were plated as single cells in medium containing puromycin supplemented with stem cell factor, IL-3, IL-6, and thrombopoietin with or without EPO. After 12–14 days, colonies were stained with antibodies recognizing glycophorin A and CD41a (markers of erythroid and megakaryotic differentiation, respectively). Colonies were classified as megakaryocytic-only (CFU-Mk), erythroid-only burst forming unit (BFU-E), or megakaryocytic/erythroid (CFU-Mk/E) (Xavier-Ferrucio et al., 2018). As shown in Figure 3A, in the presence of EPO, all cultures differentiated into erythroid lineage, megakaryotic lineage, and mixed colonies. In the absence of EPO, >50% of colonies induced by EBC5-16 were BFU-E or CFU-Mk/E, consistent with its ability to induce erythroid differentiation of hHPCs. In contrast, fewer than 5% of the colonies induced by ELI-3 in the absence of EPO were BFU-E or CFU-Mk/E, comparable with control cells lacking traptamer expression. These results demonstrated that ELI-3, unlike EBC5-16, does not promote erythroid commitment and differentiation in human MEP cells. We also note that ELI-3 does not interfere with the ability of EPO to induce erythroid differentiation.

The Cytokine Receptor β-Common Subunit Is Required for ELI-3-Induced Growth Factor Independence

Because ELI-3 did not induce erythroid differentiation, we considered the possibility that ELI-3 utilized a non-canonical EPOR signaling pathway to induce growth factor independence in BaF3 cells. EPOR and βcR can constitutively associate in the absence of EPO (Brines et al., 2004). We hypothesized that ELI-3 might activate the EPOR/βcR complex to induce proliferation of BaF3/hEPOR cells. We first confirmed that βcR was endogenously expressed in BaF3 cells, consistent with published results (Sakamaki et al., 1992) (Figure S4A, bottom panel, lanes 1 and 2). We next used co-immunoprecipitation to determine if EPOR was in complex with βcR. As shown in Figure S4A (top panel, lanes 7 and 8), the anti-βcR antibody co-immunoprecipitated hEPOR from BaF3/hEPOR cells in the presence or absence of ELI-3, showing that EPOR and βcR were in a physical complex even in the absence of ELI-3.

To assess the role of βcR in ELI-3 activity, we used CRISPR-Cas9 to knockout the endogenous *Csf2rb* gene, which encodes βcR, in BaF3 cells expressing the hEPOR. BaF3/hEPOR cells were infected by lentiviruses expressing Cas9 and one of four different single guide RNAs (sgRNAs) targeting *Csf2rb*. *Csf2rb* knockout by each sgRNA in clonal cell lines was confirmed by immunoblotting with an antibody recognizing the C terminus of βcR (Figure S4B, top panel) and by deep DNA sequencing (data not shown).

The activity of ELI-3 was determined in four βcR knockout cell lines (termed BaF3/h-βcKO cells), each generated by a different sgRNA. As shown in Figures 4A and S4C, EPO and EBC5-16 induced IL-3 independence in BaF3/h-βcKO cells, demonstrating that βcR was not required for proliferation in response to these agents. In sharp contrast, ELI-3 did not induce growth factor independence in βcR knockout cells, but

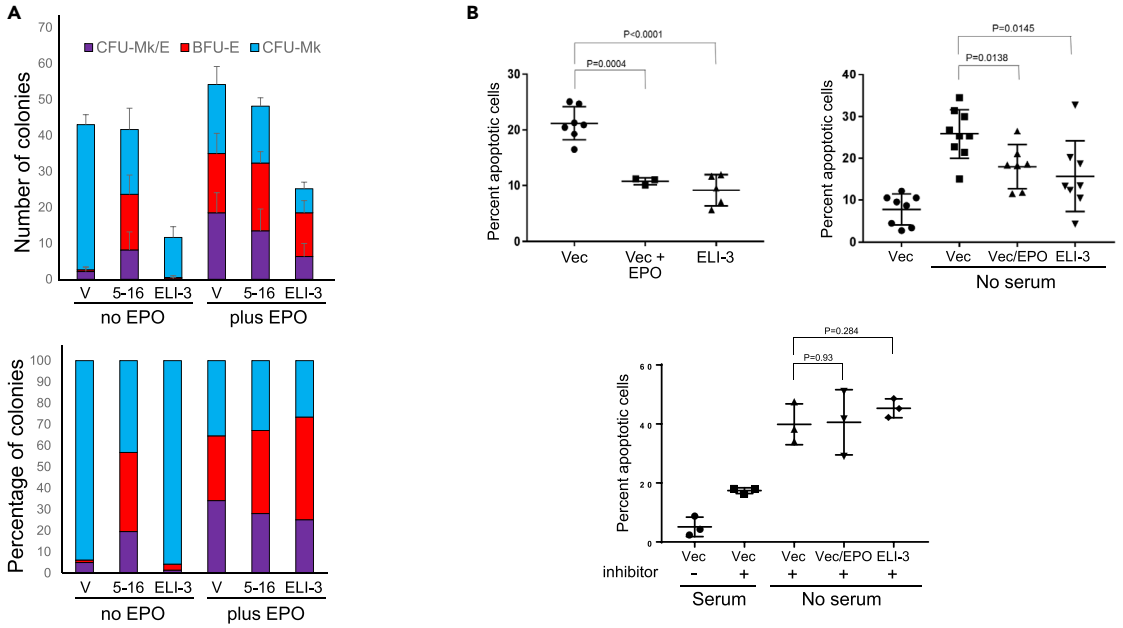

Figure 3. Biological Consequences of ELI-3-Induced EPOR Signaling

(A) Human MEP cells were infected with retrovirus expressing empty vector MSCVp (v), EBC5-16 (5–16), or ELI-3. After puromycin selection, cells were plated in medium supplemented with a cytokine cocktail with or without EPO, as indicated. After 12–14 days, the colonies were stained with anti-GpA and anti-CD41a antibodies and scored by fluorescence microscopy as megakaryocyte-only (CFU-Mk, blue), erythroid-only burst forming unit (BFU-E, red), or megakaryocyte/erythroid (CFU-Mk/E, purple). Top panel, numbers of each type of colony are shown. The averaged results and standard deviation of three independent experiments are shown. Bottom panel, the same data from top panel are shown as the relative percentage of each type of colony.

(B) Top left panel, P19 cells were infected with MSCVp empty retrovirus vector (Vec) or MSCVp expressing ELI-3. After puromycin selection, cells were plated in the presence or absence of serum for 24 h. Statistical significance was evaluated by two-tailed Student's t test with unequal variance. Where indicated, cells were treated with 2 U/mL rhEPO as described in Methods. Cells were then stained with DAPI and examined by fluorescence microscopy. Each symbol represents the fraction of cells displaying fragmented nuclei in an independent experiment. The mean ± standard deviation for each condition is shown. Top right panel, P19 cells were treated as above. Twenty-two hours later, cells were detached from the plate with trypsin, stained with fluorescein isothiocyanate-annexin V, and PI, and analyzed by flow cytometry. Each symbol represents the fraction of PI-negative cells that displayed annexin V staining in an independent experiment. The mean ± standard deviation for each condition is shown. Bottom panel, P19 cells were treated as above, except JAK2 inhibitor IV was added where indicated at time of starvation. Cells were analyzed by flow cytometry as mentioned above.

See also Figure S7.

re-expression of wild-type βcR in the knockout cells rescued the activity of ELI-3 (Figure 4A). These results demonstrate that βcR is necessary for ELI-3-induced cell proliferation.

The Cytoplasmic Tyrosines of hEPOR Are Not Required for ELI-3-Induced Cell Proliferation but the Cytoplasmic and Transmembrane Domains of the βcR Are Required

We next identified elements in hEPOR and βcR required for ELI-3-induced growth factor independence. The cytoplasmic domain of the hEPOR contains eight conserved tyrosines that are phosphorylated by JAK2 in response to EPO and serve as docking sites for signaling proteins. To determine whether ELI-3 required these tyrosines, we constructed an F8 hEPOR mutant in which all of them were mutated to phenylalanines. Parental BaF3 cells, BaF3/hEPOR cells, and BaF3/F8 cells expressing MSCVpuro, EBC5-16, or ELI-3 were cultured in the absence of IL-3 (Figure 4B). As expected, in all cases parental BaF3 cells died and BaF3/hEPOR cells incubated with EPO or expressing either traptamer grew robustly. BaF3/F8 cells grew poorly in response to EPO or EBC5-16, also as expected. Surprisingly, ELI-3 induced robust factor-independent growth of BaF3/F8 cells, indicating that ELI-3-induced mitogenic signaling did not require the conserved cytoplasmic tyrosines in the EPOR. In addition to the eight conserved tyrosines, the hEPOR cytoplasmic domain contains a non-conserved tyrosine at position 285 (Arcasoy and Karayal, 2005). We also tested whether ELI-3 conferred growth factor independence in cells expressing the F9 mutant, in which tyr285 in F8 was replaced with phenylalanine. As shown in Figure 4B, BaF3/F9 cells grew robustly in response to ELI-3, showing that tyr285 was also not essential for ELI-3 activity.

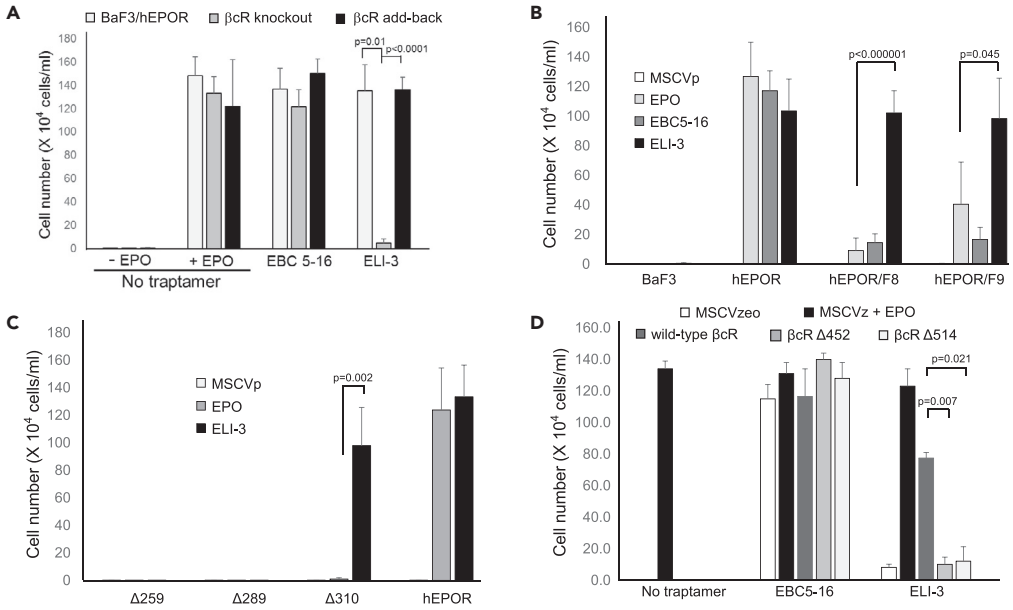

Figure 4. ELI-3-Induced Growth Factor Independence Requires βcR, but Not Cytoplasmic Domain of hEPOR

(A) BaF3/hEPOR cells, BaF3/h-βcKO cells (expressing hEPOR but knocked-out for βcR [βcR knockout]), and BaF3/h-βcKO cells reconstituted with the wild-type βcR gene (βcR add-back) were infected with empty MSCVhyg vector (no traptamer) or MSCVhyg expressing EBC5-16 or ELI-3. After hygromycin selection, cells were incubated in medium lacking IL-3, and the number of live cells was counted 6 days after IL-3 removal. Where indicated, EPO was added. The average results and standard deviation of three independent experiments are shown. Statistical significance for all panels in this figure evaluated by two-tailed Student's t test with unequal variance.

(B) Parental BaF3 cells and cells expressing the wild-type hEPOR or hEPOR mutants lacking eight (F8) or nine (F9) cytoplasmic tyrosines were infected with retroviruses to express MSCVp, EBC5-16, or ELI-3. After puromycin selection, cells were incubated in medium lacking IL-3. Where indicated, cells expressing MSCVp were incubated in medium containing EPO. The number of live cells 4 days after IL-3 removal was counted. The averaged results and standard deviation of three independent experiments is shown.

(C) BaF3 cells expressing the wild-type hEPOR or an hEPOR truncation mutant were infected with retroviruses to express MSCVp or ELI-3. After puromycin selection, cells were incubated in medium lacking IL-3. Where indicated, cells expressing MSCVp were incubated in medium containing EPO. The number of live cells is shown 4 days after IL-3 removal. The averaged results and standard deviation of three independent experiments are shown.

(D) BaF3/h-βcKO cells were infected with $MSCV_{zeo}$ empty vector or $MSCV_{zeo}$ expressing wild-type βcR or a βcR truncation mutant. After zeocine selection, cells were infected with MSCVhyg (no traptamer) or MSCVhyg expressing EBC5-16 or ELI-3. After hygromycin selection, IL-3 independence assays were performed as in (A). Where indicated, EPO was added. See also Figures S4 and S5.

We also tested C-terminal truncation mutants of hEPOR lacking various portions of the cytoplasmic domain. As shown schematically in Figure S4D, three truncation mutants (Δ259, Δ289, and Δ310) were constructed deleting all sequences downstream of trp258, gly288, and leu309, respectively. Δ259 and Δ289 mutants are defective for JAK2 binding, whereas Δ310 retains JAK2 binding. We assessed the effect of EPO or ELI-3 in cells expressing these truncation mutants. As expected, EPO did not induce IL-3 independence in cells expressing any of the hEPOR truncation mutants (Figure 4C). Similarly, ELI-3 did not confer growth factor independence in BaF3/Δ259 or BaF3/Δ289 cells, which do not bind JAK2. Strikingly, however, ELI-3 (but not EBC5-16, data not shown) induced growth factor independence in BaF3/Δ310 cells, confirming that ELI-3, unlike EPO or EBC5-16, does not require the conserved cytoplasmic tyrosines or any other sequences downstream of position 309. These results also suggest that ELI-3 requires JAK2 binding to the EPOR. Similarly, ELI-3 cooperated with an mEPOR mutant lacking most of its cytoplasmic domain (data not shown).

We also tested whether the cytoplasmic domain or TMD of the βcR was required for ELI-3 activity. We constructed two C-terminal βcR truncation mutants, βcRΔ452 and βcRΔ514, which lacked most of the cytoplasmic domain and intracellular tyrosines of βcR (Figure S5A). Δ452 removed the JAK2-binding site, whereas Δ514 left the JAK2-binding site intact (Quelle et al., 1994; Sakamaki et al., 1992). Expression of

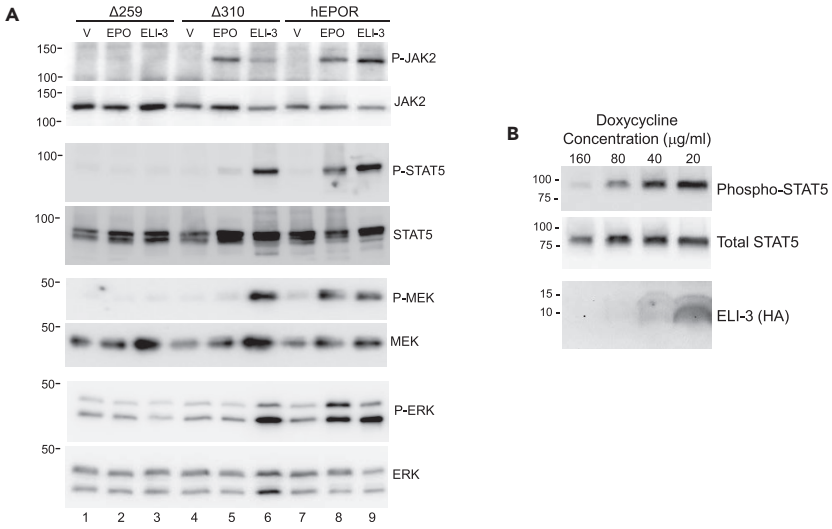

Figure 5. Cytoplasmic Tyrosines of hEPOR Are Not Required for ELI-3 Signaling

(A) Extracts were prepared from starved BaF3/Δ259, BaF3/Δ310, and BaF3/hEPOR cells expressing MSCVp (V) or ELI-3. Where indicated, cells expressing MSCVp were acutely treated with EPO. Extracts were electrophoresed and immunoblotted with anti-phospho-JAK2 (P-JAK2), anti-phospho-STAT5 (P-STAT5), anti-phospho-MEK (P-MEK), and anti-phospho-ERK1/2 (P-ERK) antibodies (top panel in each pair). Membranes were stripped and re-probed for total JAK2, STAT5, MEK, and ERK1/2 (bottom panel in each pair).

(B) BaF3 cells expressing the hEPOR and tTA tetracycline transactivator and ELI-3 expressed from a tetracycline-responsive promoter were incubated for 48 h at the indicated concentration of doxycycline and starved of IL-3 for 3 h. Extracts were electrophoresed and subjected to western blot with anti-phospho-STAT5 antibody or anti-HA antibody (to detect ELI-3). Membranes were stripped and re-probed with antibody recognizing total STAT5.

See also Figures S4 and S5.

the truncated βcR in βcR knockout cells expressing wild-type hEPOR was confirmed by blotting for the myc tag (Figure S5B, middle panel). As shown in Figure 4D, unlike wild-type βcR, the truncation mutant did not rescue the activity of ELI-3, whereas EBC5-16 activity was not affected by wild-type or mutant βcR. These results show that elements in the cytoplasmic domain of βcR are required for ELI-3 to cooperate with hEPOR to induce growth factor independence in BaF3 cells. Finally, replacing the TMD of βcR with the TMD of PDGFβR eliminated its ability to cooperate with ELI-3, even though this chimeric receptor still cooperated with EPO (Figure S6A).

ELI-3 Activates JAK2, STAT5, and Mitogen-Actiavted Protein Kinase Signaling

We next determined whether ELI-3 expression induced tyrosine phosphorylation of JAK2 and its downstream signaling proteins. BaF3/Δ259, BaF3/Δ310, and BaF3/hEPOR cells stably expressing MSCVpuro or ELI-3 were starved of IL-3 overnight and then either left untreated or acutely stimulated with 5 units/mL EPO for 5 min at 37°C. Cell lysates were subjected to SDS-polyacrylamide gel electrophoresis and immunoblotting with antibodies recognizing the phosphorylated forms of JAK2, STAT5, MEK, and ERK1/2. Membranes were then stripped and re-probed to determine the total amounts of these proteins.

As expected, JAK2 and its downstream signaling proteins STAT5, MEK and ERK1/2 were phosphorylated in response to EPO in BaF3/hEPOR cells (Figure 5A, lanes 7 and 8). In BaF3/Δ259 cells, none of these proteins were phosphorylated upon EPO treatment, because of the lack of the JAK2-binding sites on the mutant EPOR (lanes 1–3). Similarly, ELI-3 induced robust phosphorylation of JAK2 and its downstream signaling proteins in BaF3/hEPOR cells, but not in BaF3/Δ259 cells (lanes 3 and 9). Importantly, in BaF3/Δ310 cells, STAT5, MEK, and ERK1/2 were robustly phosphorylated in response to ELI-3 expression but displayed minimal phosphorylation upon EPO stimulation (Figure 5A, lanes 5 and 6). There were only minor differences in the total amounts of any of these proteins. Thus, phosphorylation of STAT5, MEK, and ERK1/2 in response to ELI-3 does not require EPOR sequences downstream of the JAK2-binding sites. JAK2 itself was phosphorylated in Δ310 cells treated with EPO or (to a lesser extent) expressing ELI-3 (Figure 5A, lanes 5 and 6).

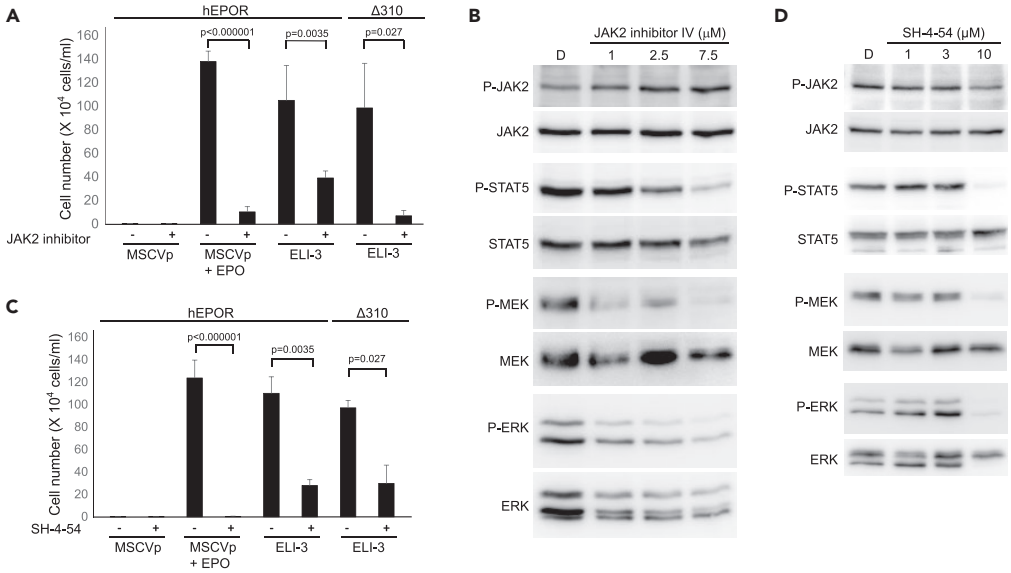

Figure 6. JAK2 and STAT Inhibitors Block ELI-3-Induced Growth Factor Independence

(A) BaF3/Δ310 and BaF3/hEPOR cells expressing MSCVp or ELI-3 were incubated in medium lacking IL-3. On day 0, cells were treated with DMSO (–) or 7.5 μM JAK2 inhibitor IV (+). Where indicated, BaF3/hEPOR cells expressing MSCVp were incubated in medium containing EPO. The number of live cells 4 days after IL-3 removal is shown. The averaged results and standard deviation of three independent experiments are shown. Statistical significance was evaluated by two-tailed Student's t test with unequal variance.

(B) BaF3/Δ310 cells expressing ELI-3 were incubated in medium lacking IL-3 for 2 h and then treated for 30 min with DMSO (D) or the indicated concentrations of JAK2 inhibitor IV. Cell extracts were electrophoresed and immunoblotted with anti-phospho-JAK2 (P-JAK2), anti-phospho-STAT5 (P-STAT5), anti-phospho-MEK (P-MEK), and anti-phospho-ERK1/2 (P-ERK) antibodies. Membranes were then stripped and re-probed for total JAK2, STAT5, MEK, and ERK1/2.

(C) Cells were treated and analyzed as in (A), except STAT5 inhibitor SH-4-54 was used.

(D) As in (B), except SH-4-54 was used.

We also expressed ELI-3 under the control of a doxycycline-regulated promoter in BaF3/hEPOR cells and tested its ability to induce STAT5 tyrosine phosphorylation. As shown in Figure 5B, ELI-3 caused a dose-dependent increase in STAT5 phosphorylation without affecting the level of total STAT5. Thus, STAT5 phosphorylation is a relatively rapid and dose-dependent response to ELI-3 expression, suggesting that it is directly induced by ELI-3.

JAK-STAT Inhibitors Inhibit ELI-3-Induced Growth Factor Independence

We used chemical inhibitors to test the importance of JAK/STAT signaling for ELI-3 activity. BaF3/hEPOR and BaF3/Δ310 cells expressing either MSCVpuro or ELI-3 were transferred to IL-3-free medium and cultured in the presence or absence of EPO. To test the requirement for JAK2, 7.5 μg/mL JAK2 inhibitor IV was added to the IL-3-free medium, and cells were counted on day 4. As expected, growth of BaF3/hEPOR cells in the presence of EPO was reduced ~90% by JAK2 inhibition (Figure 6A). JAK2 inhibition also greatly reduced the ability of ELI-3 to support growth factor-independent growth in BaF3/Δ310 cells and, to a lesser extent, in BaF3/hEPOR cells. ELI-3 activity was also inhibited by JAK inhibitor I (data not shown).

We next determined the effect of the JAK2 inhibitor on phosphorylation of downstream signaling proteins. BaF3/Δ310 cells expressing ELI-3 were starved overnight in IL-3-free medium, and then treated with either DMSO or JAK2 inhibitor IV for 3 hours. Cell lysates were analyzed by immunoblotting with antibodies recognizing phosphorylated JAK2, STAT5, MEK, and ERK1/2. As shown in Figure 6B, the JAK2 inhibitor did not inhibit JAK2 phosphorylation but caused dose-dependent reduction in phosphorylation of STAT5, MEK, and ERK. The total amounts of these proteins were largely unaffected by the inhibitor. These data indicated that the JAK2 activity is important for ELI-3 signaling.

Similarly, cells were treated with 3 μM SH-4-54, a STAT3/5 inhibitor. As expected, growth of the BaF3/hEPOR cells cultured in IL-3-free medium containing EPO was abolished by SH-4-54 (Figure 6C). ELI-3-induced growth

in the absence of IL-3 was reduced by ~80% in BaF3/hEPOR or BaF3/Δ310 cells, suggesting an important, but not absolute, requirement for STAT5 in ELI-3-induced cell proliferation. Figure 6D showed that STAT5 inhibition greatly reduced the phosphorylation of STAT5, MEK, and ERK in BaF3/hEPOR cells without affecting the overall abundance of these proteins, suggesting that STAT5 is upstream of the mitogen-activated protein kinase pathway in ELI-3-induced signaling.

Requirements for Complex Formation between ELI-3, hEPOR, and βcR

To explore the requirement for assembly of a signaling complex, we first showed that the EPOR truncation mutants constitutively associated with βcR (Figure S4A, top panel). Thus, hEPOR sequences downstream of trp258, including the JAK2-binding sites, were not required for this interaction. Similarly, the Δ452 cytoplasmic truncation mutant of βcR retained the ability to form a complex with hEPOR (Figure S5C). In contrast, heteroreceptor formation was inhibited by replacing the TMD of either hEPOR or βcR with a foreign TMD (Figures S6B and S6C).

To determine if βcR was required for complex formation between ELI-3 and EPOR, we expressed MSCVpuro or F-ELI-3 in BaF3, BaF3/h-βcKO, and BaF3/hEPOR cells. Protein extracts were immunoprecipitated with anti-FLAG antibodies and immunoblotted with antibodies recognizing the HA epitope on hEPOR. As expected, anti-FLAG antibodies co-immunoprecipitated little hEPOR in cells lacking ELI-3 expression, presumably due to non-specific sticking of EPOR to the anti-FLAG beads (Figure 7A, lanes 1 and 3). In contrast, anti-FLAG antibodies co-immunoprecipitated abundant hEPOR from cells expressing F-ELI-3, whether or not the βcR was present (Figure 7A, lanes 4 and 6), showing that complex formation between ELI-3 and the hEPOR did not require the βcR.

We also determined whether ELI-3 and βcR were in a complex. Anti-FLAG immunoprecipitates were immunoblotted with an antibody recognizing the βcR. As shown in Figure 7B, anti-FLAG immunoprecipitated a small amount of βcR from cells expressing hEPOR (lane 6), but not from cells that did not express hEPOR (lane 5). The βcR antibody also reacted with a major non-specific band migrating at ~120 kDa in the immunoprecipitated samples, even in the βcR knockout cells. These results indicated that ELI-3 and the βcR are present in a stable complex and that complex formation required co-expression of the hEPOR.

βcR and hEPOR Are Mutually Required for Signaling in Response to ELI-3

To examine βcR phosphorylation, lysates prepared from parental BaF3 cells, BaF3/hEPOR cells, and BaF3/h-βcKO cells were immunoprecipitated with anti-βcR antibody and immunoblotted with a broadly reactive anti-phosphotyrosine antibody. As expected, βcR was phosphorylated at only a low level in cells expressing MSCVhyg in the presence or absence of EPO treatment (Figure 7C, lanes 1 and 2), but was phosphorylated in cells stimulated with IL-3 (Figure 7C, lane 3). Importantly, phosphorylation of βcR was also observed in cells co-expressing ELI-3, hEPOR, and βcR (Figure 7C, lane 4), but not in cells expressing ELI-3 in the absence of hEPOR (Figure 7C, lane 6), indicating that the hEPOR was required for ELI-3-induced βcR activation. Furthermore, ELI-3 did not induce βcR tyrosine phosphorylation in cells expressing hEPOR/Δ259 (Figure 7D, lane 4), suggesting that the JAK2-binding boxes on hEPOR were required for βcR phosphorylation in response to ELI-3 (but not in response to IL-3 [Figure 7D, lane 3]). Even though the cytoplasmic tyrosines of EPOR are not required for ELI-3 activity, phosphotyrosine blotting showed that ELI-3 induced phosphorylation of hEPOR, but only when βcR was co-expressed (Figure 7E, lanes 4 and 5).

We also examined phosphorylation of downstream signaling proteins. Extracts were prepared from IL-3-starved cells (treated, where indicated, with EPO). ELI-3 induced phosphorylation of JAK2, STAT5, MEK, and ERK1/2 in cells with intact βcR (Figure 7F, lane 4), but phosphorylation was eliminated in all four βcR knockout cell lines (Figure 7F, lanes 6 and 8, and data not shown). βcR knockout did not affect phosphorylation induced by EBC5-16 (Figure 7F, lanes 5 and 7). Thus, downstream signaling by ELI-3 required βcR.

ELI-3 Confers Tissue Protection

Finally, we assessed the tissue protection activity of ELI-3 in mouse P19 teratocarcinoma cells, which undergo apoptosis when cultured in medium lacking serum (Galli and Fratelli, 1993; Siren et al., 2001a). Apoptosis is reduced by treating the cells with high concentrations of EPO or with EPO derivatives that activate the EPOR/βcR heteroreceptor (Erbayraktar et al., 2003). Here, we removed serum from P19 cells expressing ELI-3 or MSCVpuro. Twenty-four hours later, nuclei were stained with DAPI and cells were examined by fluorescence microscopy. As shown in Figure 3B, top left panel, ~20% of control cells lacking ELI-3

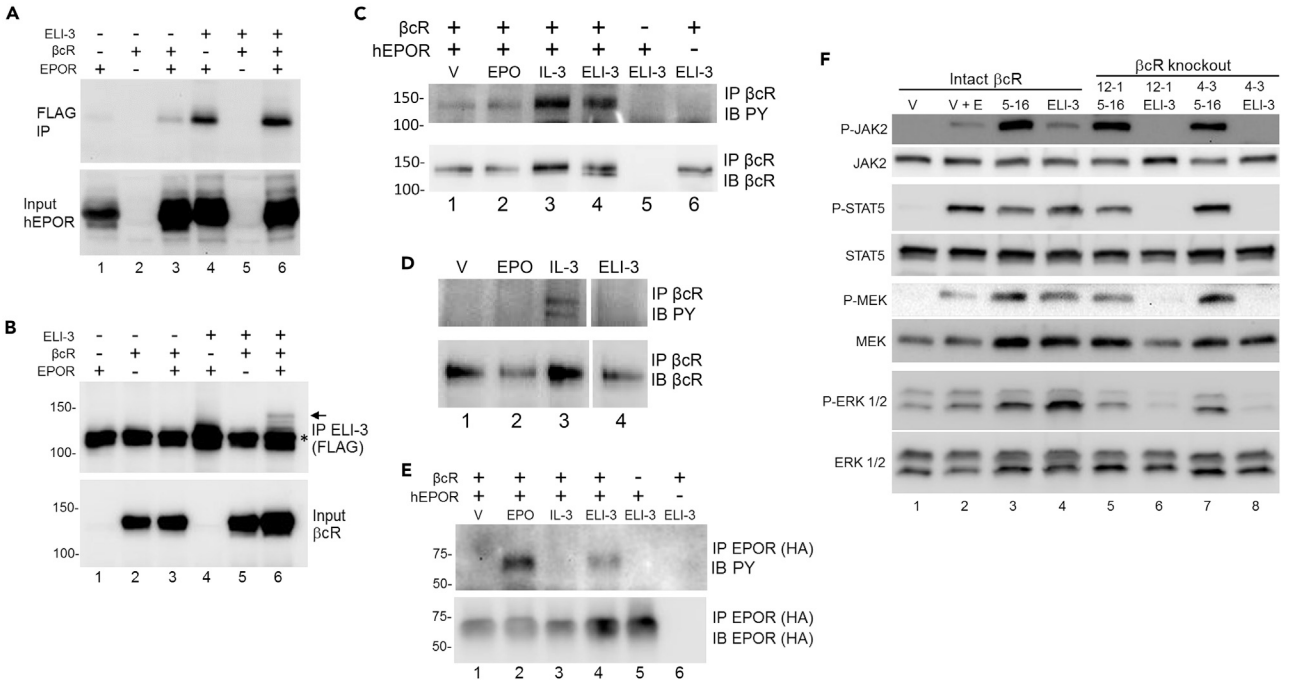

Figure 7. EPOR and βcR Requirements for Complex Formation and Signaling

(A and B) Extracts prepared from BaF3, BaF3/h-βcKO (clone 12-1), and BaF3/hEPOR cells expressing MSCVhyg or F-ELI-3 were immunoprecipitated with anti-FLAG magnetic beads (FLAG IP) or directly subjected to gel electrophoresis (input). The membranes were immunoblotted with anti-HA antibody to probe for hEPOR (A) or with anti-βcR antibody (B). Arrow in (B) indicates the band of co-immunoprecipitated βcR. Non-specific bands at ~120 kDa are marked with an asterisk.

(C) Extracts were prepared from IL-3-starved BaF3 cells (lane 6), BaF3/hEPOR cells (lanes 1 to 4), and BaF3/h-βcKO cells (clone 12-1) (lane 5) expressing MSCVhyg (V) or ELI-3. Where indicated, BaF3/hEPOR cells expressing MSCVhyg were also acutely treated with EPO or IL-3. Extracts were immunoprecipitated with anti-βcR antibody and immunoblotted with anti-phosphotyrosine antibody PY100 (top panel). The same membrane was stripped and re-probed with anti-βcR antibody (bottom panel).

(D) Extracts prepared from starved BaF3/Δ259 cells expressing MSCVhyg vector (lanes 1–3) or ELI-3 (lane 4) were immunoprecipitated with anti-βcR antibody and immunoblotted with anti-phosphotyrosine antibody (top panels). Cells were treated with EPO or IL-3 as indicated. Membranes were stripped and re-probed with anti-βcR antibody (bottom panel). An irrelevant lane was excised as indicated (between lanes 3 and 4).

(E) Extracts were prepared from IL-3-starved BaF3/hEPOR (lanes 1–4), BaF3/h-βcKO (lane 5), and parental BaF3 (lane 6) cells expressing ELI-3, treated with EPO or IL-3, or left untreated, as indicated. Extracts were immunoprecipitated with anti-HA to precipitate hEPOR and then blotted with anti-phosphotyrosine antibody (top panel) or with anti-HA antibody to visualize tyrosine-phosphorylated or total hEPOR (bottom panel).

(F) Extracts prepared from starved BaF3/hEPOR (intact βcR) and the indicated clonal BaF3/h-βcKO cells expressing MSCVhyg (V) or ELI-3 were immunoblotted with anti-phospho-JAK2 (P-JAK2), anti-phospho-STAT5 (P-STAT5), anti-phospho-MEK (P-MEK), and anti-phospho-ERK1/2 (P-ERK) antibodies (top panels in each pair). In lane 2, BaF3/hEPOR cells expressing MSCVhyg were also acutely treated with EPO. The membranes were then stripped and re-probed for the total JAK2, STAT5, MEK, and ERK1/2 (bottom panels).

expression underwent apoptosis in the absence of EPO, as assessed by nuclear fragmentation. Consistent with published reports, 2 U/mL EPO caused an ~50% reduction in apoptosis. P19 cells expressing ELI-3 in the absence of EPO were protected against apoptosis to a similar extent. We also used flow cytometry for annexin V staining to test the ability of ELI-3 to protect P19 cells from apoptosis. Cells treated as above were stained with annexin V and propidium iodide (PI) and analyzed by flow cytometry. Apoptotic cells were scored as cells showing annexin V staining to the outer leaflet of the plasma membrane in the absence of PI uptake (Figure S7). As shown in Figure 3B, top right panel, EPO and ELI-3 caused about a 2-fold reduction in apoptotic cells in this assay as well. JAK2 inhibitor IV abrogated the ability of EPO or ELI-3 to protect cells (Figure 3B, bottom panel). These results showed that ELI-3 can protect non-hematopoietic cells from stress-induced apoptosis and suggest that protection requires JAK2 activity.

DISCUSSION

Although EPO is best known for its role in erythropoiesis, it can activate distinct EPOR complexes with different biological outcomes. A homodimeric form of the EPOR binds EPO with high affinity and drives

production of red blood cells, and a heteromeric complex containing both the EPOR and the βcR binds EPO with lower affinity, is inactive in erythropoiesis, and appears to mediate tissue protection. The molecular basis underlying cooperation between the EPOR and βcR deserves attention because induction of the tissue protective response may provide opportunities to limit tissue damage following injury, but little is known about how the heteroreceptor complex forms or initiates signaling. We report here the characterization of a small TM protein that induces EPOR/βcR signaling by interacting with the TMD of the EPOR. We demonstrated that most of the cytoplasmic domain of the EPOR is not required for heteroreceptor signaling in response to ELI-3 and identified elements in EPOR and βcR that are required for formation of the heteroreceptor.

Both ELI-3 and EBC5-16 target the EPOR TMD and induce growth factor independence in BaF3 cells, but they have completely different hydrophobic sequences and use fundamentally different mechanisms to trigger EPOR signaling. EBC5-16, like EPO, required cytoplasmic tyrosines on the EPOR, was independent of βcR, and supported erythropoiesis *in vitro*, whereas ELI-3 was active in the absence of these tyrosines but required βcR as well as hEPOR, failed to induce erythroid differentiation, and conferred tissue protection. ELI-3 induced phosphorylation of EPOR and downstream substrates only if βcR is present, indicating that ELI-3 does not cause productive EPOR homodimerization, consistent with its lack of erythropoietic activity. Although hEPOR can productively couple to murine βcR, we have not tested whether hEPOR can cooperate with human βcR to mediate ELI-3 activity. In addition to βcR, mouse cells express a closely related IL-3-specific β-chain receptor, but the inability of βcR knockout cells to respond to ELI-3 indicates that the IL-3-specific isoform cannot cooperate with hEPOR to support ELI-3-induced proliferation or signaling in BaF3 cells.

This work provides important new insight into cooperative signaling by the EPOR and βcR. First, little if any of the cytoplasmic domain of either receptor is required for heteroreceptor formation in the absence of ELI-3, but the TMDs of both proteins are required. In addition, the extracellular domains of the EPOR and βcR do not physically interact *in vitro* (Cheung Tung Shing et al., 2018). These findings suggest that the TMD and/or the TMD-proximal segments of the EPOR and βcR mediate heteroreceptor formation. Second, EPOR/βcR signaling can be activated by proteins that interact non-covalently with the TMD of EPOR, in contrast to previously known activators of this complex, which bind to the ligand-binding domain (Brines et al., 2004). Third, productive signaling is dependent on the intracellular domain of βcR and intact JAK2-binding sites on the EPOR. Importantly, EPOR/βcR-mediated proliferation induced by ELI-3 does not require phosphorylated tyrosines or most of the cytoplasmic domain of the EPOR. Previous reports studying phosphotyrosine-null mutants of EPOR suggested that the receptor can initiate phosphotyrosine-independent signaling. Yoon and Watowich showed that EPOR can provide a phosphotyrosine-independent survival signal in 32D cells (Yoon and Watowich, 2003), and EPOR-HM, a mutant removing all cytoplasmic tyrosines, induced attenuated signaling in primary hematopoietic progenitor cells (Li et al., 2003). Mice expressing EPOR-HM maintained steady-state erythropoiesis but were impaired for stress erythropoiesis (Menon et al., 2006; Zang et al., 2001). It has been proposed that STAT5 can bind directly to phosphorylated JAK2 bound to EPOR to mediate some of these responses (Fujitani et al., 1997), but the role of βcR in these situations was not assessed.

Complex formation between ELI-3 and EPOR does not require βcR, and ELI-3 does not associate with βcR in the absence of the EPOR. In addition, ELI-3 does not interact with EPOR containing a foreign TMD and point mutations in the EPOR TMD can inhibit ELI-3 activity. Finally, our NMR experiments conducted in the absence of other protein components suggest that peptides composed of ELI-3 and hEPOR TMD interact *in vitro*. Taken together, these findings suggest that ELI-3 and the EPOR TMD contact one another directly, as has been shown for other small TM proteins that activate the hEPOR or PDGFβR (Edwards et al., 2013; He et al., 2017).

After GM-CSF binds to the GM-CSF receptor α-chain in complex with βcR, JAK2 associated with βcR phosphorylates multiple cytoplasmic tyrosines on βcR that then serve as docking sites for signaling factors, including STAT5 (Brizzi et al., 1994; Quelle et al., 1994; Sakamaki et al., 1992). Based on structural and biochemical studies of GM-CSFR, Hansen et al. proposed that the active GM-CSFR/βcR heteroreceptor is a dodecameric structure containing four βcR molecules, four GM-CSFR molecules, and four molecules of GM-CSF ligand (Hansen et al., 2008). This complicated architecture appears to be required to bring two JAK2 molecules into juxtaposition to autophosphorylate because GM-CSFR itself does not contain JAK2-binding sites, and the JAK2 sites in a βcR dimer are otherwise too far apart to allow

autophosphorylation (Carr et al., 2001). EPOR/βcR heteroreceptor signaling does not necessarily require this complex arrangement, because hEPOR itself contains JAK2-binding sites, which are required for ELI-3 signaling. Furthermore, the EPOR/βcR heteroreceptor does not utilize the cytoplasmic tyrosines in the EPOR to signal, suggesting that the overall architecture of the EPOR/βcR signaling complex is profoundly different from the active EPOR homodimer.

We propose that the TMD of ELI-3 binds directly to the TMD of EPOR in the EPOR/βcR heteroreceptor and that ELI-3 binding recruits another EPOR molecule into the complex or causes a conformational change in the EPOR/βcR heteroreceptor. This allows JAK2 to autophosphorylate and phosphorylate tyrosines in the cytoplasmic domain of βcR, thereby generating the docking platform that assembles the signaling complex. Consistent with this model, ELI-3-induced phosphorylation of the receptors and downstream substrates requires both EPOR and βcR, and the membrane-distal cytoplasmic segment of βcR, but not EPOR, is required for ELI-3 activity. Thus, signaling in response to ELI-3 requires true cooperation between EPOR and βcR: EPOR provides the binding site for ELI-3 as well as required JAK2-binding sites, and βcR provides tyrosines to serve as docking sites. Further analysis of the ability of additional EPOR and βcR mutants to support ELI-3 action is required to refine and test this model.

EPOR/βcR heteroreceptor signaling has previously been implicated in the tissue-protective effects of EPO (Bohr et al., 2015; Brines et al., 2004; Kahn et al., 2013; reviewed in Brines, 2010). Our results confirm that the activated EPOR/βcR complex lacks erythropoietic activity but confers tissue protection. In this regard, ELI-3 is similar to carbamylated EPO and short fragments of EPO that activate EPOR/βcR signaling and confer tissue protection but do not induce erythropoiesis. It is not clear whether EPOR/βcR signaling induced by ELI-3 is the same as that induced by soluble molecules that bind to the extracellular domain of the EPOR, or whether ELI-3 has revealed the existence of a previously unknown EPOR output.

Our inhibitor studies indicate that JAK2/STAT5 signaling is important for growth factor independence and tissue protection in response to ELI-3. EPO also activates additional signaling pathways, including GATA1 and nuclear factor-κB signaling, some of which have been implicated in the tissue-protective effects of EPO (e.g., Digicaylioglu and Lipton, 2001). Further analysis of signaling induced by ELI-3 and EBC5-16 will determine whether these pathways are triggered by traptamers and provide new insights into the signal transduction pathways that mediate these important cellular responses.

This work also highlights the power of specific TM interactions to regulate cell behavior. We show here that specific TM interactions involving different traptamers with the same target TMD can activate different receptor complexes. We previously showed that the ability of traptamers to distinguish between the hEPOR and the mEPOR can be determined by differences as minimal as the position of a single side-chain methyl group in a traptamer (He et al., 2017). The chemical basis for the ability of traptamers to distinguish between closely related targets and to activate different receptor complexes remains to be determined.

Limitations of the Study

Further experiments are required to establish whether ELI-3 binds directly to the EPOR TM domain, refine the model of EPOR/βcR heteromeric receptor activation, and determine the signaling pathways required for ELI-3-induced tissue protection and proliferation.

METHODS

All methods can be found in the accompanying Transparent Methods supplemental file.

SUPPLEMENTAL INFORMATION

Supplemental Information can be found online at https://doi.org/10.1016/j.isci.2019.06.027.

ACKNOWLEDGMENTS

We thank Michael Hinrichsen and Susan Jun for help with preliminary experiments. We thank Rakesh Verma for helpful comments, Yarden Opatowsky for help with graphics, and Jan Zulkeski for assistance in preparing this manuscript. E.B.C. was supported in part by F31 grant CA0168012 from the NCI. This work was supported by NIDDK grant U54DK106857 to D.S.K. and NCI grant CA037157 to D.D.

AUTHOR CONTRIBUTIONS

Conceptualization, L.H., E.B.C., B.B.K., D.S.K., and D.D.; Methodology, L.H., E.B.C., J.X.F., D.A., R.M.M., R.S.F., and K.O.B; Investigation, L.H., E.B.C., J.X.F., D.A., R.S.F., and K.O.B; Writing—Original Draft, L.H. and D.D; Writing—Review and Editing, L.H., E.B.C., J.X.F., K.O.B., B.B.K., D.S.K., and D.D; Funding Acquisition, E.B.C., D.S.K., and D.D; Resources, R.M.M., D.S.K., and D.D; Supervision, B.B.K., D.S.K., and D.D.

DECLARATION OF INTERESTS

The authors declare no competing interests.

Received: January 16, 2019
Revised: May 10, 2019
Accepted: June 17, 2019
Published: July 26, 2019

REFERENCES

Acharya, R., Carnevale, V., Fiorin, G., Levine, B.G., Polishchuk, A.L., Balannik, V., Samish, I., Lamb, R.A., Pinto, L.H., Degrado, W.F., and Klein, M.L. (2010). Structure and mechanism of proton transport through the transmembrane tetrameric M2 protein bundle of the influenza A virus. Proc. Natl. Acad. Sci. U S A *107*, 15075–15080.

Arcasoy, M.O., and Karayal, A.F. (2005). Erythropoietin hypersensitivity in primary familial and congenital polycythemia: role of tyrosines Y285 and Y344 in erythropoietin receptor cytoplasmic domain. Biochim. Biophys. Acta *1740*, 17–28.

Barber, D.L., Corless, C.N., Xia, K., Roberts, T.M., and D'Andrea, A.D. (1997). Erythropoietin activates Raf1 by an Shc-independent pathway in CTLL-EPO-R cells. Blood *89*, 55–64.

Blake, T.J., Jenkins, B.J., D'Andrea, R.J., and Gonda, T.J. (2002). Functional cross-talk between cytokine receptors revealed by activating mutations in the extracellular domain of the B-subunit of the GM-CSF receptor. J. Leukoc. Biol. *72*, 1246–1255.

Bohr, S., Patel, S.J., Vasko, R., Shen, K., Iracheta-Vellve, A., Lee, J., Bale, S.S., Chakraborty, N., Brines, M., Cerami, A., et al. (2015). Modulation of cellular stress response via the erythropoietin/CD131 heteroreceptor complex in mouse mesenchymal-derived cells. J. Mol. Med. (Berl.) *93*, 199–210.

Brines, M. (2010). The therapeutic potential of erythropoiesis-stimulating agents for tissue protection: a tale of two receptors. Blood Purif. *29*, 86–92.

Brines, M., Grasso, G., Fiordaliso, F., Sfacteria, A., Ghezzi, P., Fratelli, M., Latini, R., Xie, Q.W., Smart, J., Su-Rick, C.J., et al. (2004). Erythropoietin mediates tissue protection through an erythropoietin and common beta-subunit heteroreceptor. Proc. Natl. Acad. Sci. U S A *101*, 14907–14912.

Brizzi, M.F., Zini, M.G., Aronica, M.G., Blechman, J.M., Yarden, Y., and Pegoraro, L. (1994). Convergence of signaling by interleukin-3, granulocyte-macrophage colony-stimulating factor, and mast cell growth factor on JAK2 tyrosine kinase. J. Biol. Chem. *269*, 31680–31684.

Cammett, T.J., Jun, S.J., Cohen, E.B., Barrera, F.N., Engelman, D.M., and DiMaio, D. (2010). Construction and genetic selection of small transmembrane proteins that activate the human erythropoietin receptor. Proc. Natl. Acad. Sci. U S A *107*, 3447–3452.

Carr, P.D., Gustin, S.E., Church, A.P., Murphy, J.M., Ford, S.C., Mann, D.A., Woltring, D.M., Walker, I., Ollis, D.L., and Young, I.G. (2001). Structure of the complete extracellular domain of the common beta subunit of the human GM-CSF, IL-3, and IL-5 receptors reveals a novel dimer configuration. Cell *104*, 291–300.

Cheung Tung Shing, K.S., Broughton, S.E., Nero, T.L., Gillinder, K., Ilsley, M.D., Ramshaw, H., Lopez, A.F., Griffin, M.D.W., Parker, M.W., Perkins, A.C., and Dhagat, U. (2018). EPO does not promote interaction between the erythropoietin and beta-common receptors. Sci. Rep. *8*, 12457.

Cohen, E.B., Jun, S.J., Bears, Z., Barrera, F.N., Alonso, M., Engelman, D.M., and DiMaio, D. (2014). Mapping the homodimer interface of an optimized, artificial, transmembrane protein activator of the human erythropoietin receptor. PLoS One *9*, e95593.

Constantinescu, S.N., Ghaffari, S., and Lodish, H.F. (1999a). The erythropoietin receptor: structure, activation and intracellular signal transduction. Trends Endocrinol. Metab. *10*, 18–23.

Constantinescu, S.N., Huang, L.J.-S., Nam, H.-S., and Lodish, H.F. (2001). The erythropoietin receptor cytosolic juxtamembrane domain contains an essential, precisely oriented, hydrophobic motif. Mol. Cell *7*, 377–385.

Constantinescu, S.N., Liu, X., Beyer, W., Fallon, A., Shekar, S., Henis, Y.I., Smith, S.O., and Lodish, H.F. (1999b). Activation of the erythropoietin receptor by the $gp^{55\text{-}P}$ viral envelope protein is determined by a single amino acid in its transmembrane domain. EMBO J. *18*, 3334–3347.

Digicaylioglu, M., and Lipton, S.A. (2001). Erythropoietin-mediated neuroprotection involves cross-talk between Jak2 and NF-kappaB signalling cascades. Nature *412*, 641–647.

DiMaio, D., and Petti, L.M. (2013). The E5 proteins. Virology *445*, 99–114.

Edwards, A.P., Xie, Y., Bowers, L., and DiMaio, D. (2013). Compensatory mutants of the bovine papillomavirus E5 protein and the platelet-derived growth factor beta receptor reveal a complex direct transmembrane interaction. J. Virol. *87*, 10936–10945.

Erbayraktar, S., Grasso, G., Sfacteria, A., Xie, Q.W., Coleman, T., Kreilgaard, M., Torup, L., Sager, T., Erbayraktar, Z., Gokmen, N., et al. (2003). Asialoerythropoietin is a nonerythropoietic cytokine with broad neuroprotective activity in vivo. Proc. Natl. Acad. Sci. U S A *100*, 6741–6746.

Erbayraktar, Z., Erbayraktar, S., Yilmaz, O., Cerami, A., Coleman, T., and Brines, M. (2009). Nonerythropoietic tissue protective compounds are highly effective facilitators of wound healing. Mol. Med. *15*, 235–241.

Freeman-Cook, L., Dixon, A.M., Frank, J.B., Xia, Y., Ely, L., Gerstein, M., Engelman, D.M., and DiMaio, D. (2004). Selection and characterization of small random transmembrane proteins that bind and activate the platelet-derived growth factor beta receptor. J. Mol. Biol. *338*, 907–920.

Freeman-Cook, L.L., and DiMaio, D. (2005). Modulation of cell function by small transmembrane proteins modeled on the bovine papillomavirus E5 protein. Oncogene *24*, 7756–7762.

Fujitani, Y., Hibi, M., Fukada, T., Takahashi-Tezuka, M., Yoshida, H., Yamaguchi, T., Sugiyama, K., Yamanaka, Y., Nakajima, K., and Hirano, T. (1997). An alternative pathway for STAT activation that is mediated by the direct interaction between JAK and STAT. Oncogene *14*, 751–761.

Galli, G., and Fratelli, M. (1993). Activation of apoptosis by serum deprivation in a teratocarcinoma cell line: inhibition by L-acetylcarnitine. Exp. Cell Res. *204*, 54–60.

Hansen, G., Hercus, T.R., McClure, B.J., Stomski, F.C., Dottore, M., Powell, J., Ramshaw, H., Woodcock, J.M., Xu, Y., et al. (2008). The structure of the GM-CSF receptor complex reveals a distinct mode of cytokine receptor activation. Cell *134*, 496–507.

He, L., Steinocher, H., Shelar, A., Cohen, E.B., Heim, E.N., Kragelund, B.B., Grigoryan, G., and

DiMaio, D. (2017). Single methyl groups can act as toggle switches to specify transmembrane protein-protein interactions. Elife *6*, e27701.

Hercus, T.R., Dhagat, U., Kan, W.L., Broughton, S.E., Nero, T.L., Perugini, M., Sandow, J.J., D'Andrea, R.J., Ekert, P.G., Hughes, T., et al. (2013). Signalling by the beta c family of cytokines. Cytokine Growth Factor Rev. *24*, 189–201.

Jelkmann, W., Depping, R., and Metzen, E. (2009). Nonhematopoietic effects of erythropoiesis-stimulating agents. In Erythropoietins, Erythropoietic Factors and Erythropoiesis, Second Edition, S.G. Elliott, M.A. Foote, and G. Molineux, eds. (Birkhäuser), pp. 299–317.

Jubinsky, P.T., Krijanovski, O.I., Nathan, D.G., Tavernier, J., and Sieff, C.A. (1997). The beta chain of the interleukin-3 receptor functionally associates with the erythropoietin receptor. Blood *90*, 1867–1873.

Kahn, J.A., Xu, J., Kapogiannis, B.G., Rudy, B., Gonin, R., Liu, N., Wilson, C.M., Worrell, C., and Squires, K.E. (2013). Immunogenicity and safety of the human papillomavirus 6, 11, 16, 18 vaccine in HIV-infected young women. Clin. Infect Dis. *57*, 735–744.

Kovacs, E., Zorn, J.A., Huang, Y., Barros, T., and Kuriyan, J. (2015). A structural perspective on the regulation of the epidermal growth factor receptor. Annu. Rev. Biochem. *84*, 739–764.

Kuhrt, D., and Wojchowski, D.M. (2015). Emerging EPO and EPO receptor regulators and signal transducers. Blood *125*, 3536–3541.

Leist, M., Ghezzi, P., Grasso, G., Bianchi, R., Villa, P., Fratelli, M., Savino, C., Bianchi, M., Nielsen, J., Gerwien, J., et al. (2004). Derivatives of erythropoietin that are tissue protective but not erythropoietic. Science *305*, 239–242.

Li, J.-P., D'Andrea, A.D., Lodish, H.F., and Baltimore, D. (1990). Activation of cell growth by binding of Friend spleen focus-forming virus gp55 glycoprotein to the erythropoietin receptor. Nature *343*, 762–764.

Li, K., Menon, M.P., Karur, V.G., Hegde, S., and Wojchowski, D.M. (2003). Attenuated signaling by a phosphotyrosine-null Epo receptor form in primary erythroid progenitor cells. Blood *102*, 3147–3153.

Li, Q., Wong, Y.L., Lee, M.Y., Li, Y., and Kang, C. (2015). Solution structure of the transmembrane domain of the mouse erythropoietin receptor in detergent micelles. Sci. Rep. *5*, 13586.

Lodish, H.F., Ghaffari, S., Socolovsky, M., Tong, W., and Zhang, J. (2009). Intracellular signaling by the erythropoietin receptor. In Erythropoietins, Erythropoietic Factors and Erythropoiesis, Second Edition, S.G. Elliott, M.A. Foote, and G. Molineux, eds. (Birkhäuser), pp. 155–173.

Lopez, A.F., Elliott, M.J., Woodcock, J., and Vadas, M.A. (1992). GM-CSF, IL-3 and IL-5: cross-competition on human haemopoietic cells. Immunol. Today *13*, 495–500.

Menon, M.P., Karur, V., Bogacheva, O., Bogachev, O., Cuetara, B., and Wojchowski, D.M. (2006). Signals for stress erythropoiesis are integrated via an erythropoietin receptor-phosphotyrosine-343-Stat5 axis. J. Clin. Invest. *116*, 683–694.

Murphy, J.M., and Young, I.G. (2006). IL-3, IL-5, and GM-CSF signaling: crystal structure of the human beta-common receptor. Vitam. Horm. *74*, 1–30.

Petti, L., and DiMaio, D. (1992). Stable association between the bovine papillomavirus E5 transforming protein and activated platelet-derived growth factor receptor in transformed mouse cells. Proc. Natl. Acad. Sci. U S A *89*, 6736–6740.

Petti, L., Nilson, L.A., and Dimaio, D. (1991). Activation of the platelet-derived growth factor receptor by the bovine papillomavirus E5 transforming protein. EMBO J. *10*, 845–855.

Quelle, F.W., Sato, N., Witthuhn, B.A., Inhorn, R.C., Eder, M., Miyajima, A., Griffin, J.D., and Ihle, J.N. (1994). JAK2 associates with the beta c chain of the receptor for granulocyte-macrophage colony-stimulating factor, and its activation requires the membrane-proximal region. Mol. Cell Biol. *14*, 4335–4341.

Sakamaki, K., Miyajima, I., Kitamura, T., and Miyajima, A. (1992). Critical cytoplasmic domains of the common beta subunit of the human GM-CSF, IL-3 and IL-5 receptors for growth signal transduction and tyrosine phosphorylation. EMBO J. *11*, 3541–3549.

Sanada, C., Xavier-Ferrucio, J., Lu, Y.C., Min, E., Zhang, P.X., Zou, S., Kang, E., Zhang, M., Zerafati, G., Gallagher, P.G., and Krause, D.S. (2016). Adult human megakaryocyte-erythroid progenitors are in the CD34+CD38mid fraction. Blood *128*, 923–933.

Sawyer, S.T., and Penta, K. (1996). Association of JAK2 and STAT5 with erythropoietin receptors. Role of receptor phosphorylation in erythropoietin signal transduction. J. Biol. Chem. *271*, 32430–32437.

Scheideman, E.H., Marlatt, S.A., Xie, Y., Hu, Y., Sutton, R.E., and DiMaio, D. (2012). Transmembrane protein aptamers that inhibit CCR5 expression and HIV coreceptor function. J. Virol. *86*, 10281–10292.

Siren, A.L., and Ehrenreich, H. (2001). Erythropoietin–a novel concept for neuroprotection. Eur. Arch. Psychiatry Clin. Neurosci. *251*, 179–184.

Siren, A.L., Fratelli, M., Brines, M., Goemans, C., Casagrande, S., Lewczuk, P., Keenan, S., Gleiter, C., Pasquali, C., Capobianco, A., et al. (2001a). Erythropoietin prevents neuronal apoptosis after cerebral ischemia and metabolic stress. Proc. Natl. Acad. Sci. U S A *98*, 4044–4049.

Siren, A.L., Knerlich, F., Poser, W., Gleiter, C.H., Bruck, W., and Ehrenreich, H. (2001b). Erythropoietin and erythropoietin receptor in human ischemic/hypoxic brain. Acta Neuropathol. *101*, 271–276.

Um, M., Gross, A.W., and Lodish, H.F. (2007). A "classical" homodimeric erythropoietin receptor is essential for the antiapoptotic effects of erythropoietin on differentiated neuroblastoma SH-SY5Y and pheochromocytoma PC-12 cells. Cell Signal. *19*, 634–645.

Watowich, S.S., Liu, K.D., Xie, X., Lai, S.Y., Mikami, A., Longmore, G.D., and Goldsmith, M.A. (1999). Oligomerization and scaffolding functions of the erythropoietin receptor cytoplasmic tail. J. Biol. Chem. *274*, 5415–5421.

Weber, A., Dzietko, M., Berns, M., Felderhoff-Mueser, U., Heinemann, U., Maier, R.F., Obladen, M., Ikonomidou, C., and Buhrer, C. (2005). Neuronal damage after moderate hypoxia and erythropoietin. Neurobiol. Dis. *20*, 594–600.

Xavier-Ferrucio, J., Ricon, L., Vieira, K., Longhini, A.L., Lazarini, M., Bigarella, C.L., Franchi, G., Jr., Krause, D.S., and Saad, S.T.O. (2018). Hematopoietic defects in response to reduced Arhgap21. Stem Cell Res. *26*, 17–27.

Yamanaka, K., Eldeiry, M., Aftab, M., Mares, J., Ryan, T.J., Meng, X., Weyant, M.J., Cleveland, J.C., Jr., Fullerton, D.A., and Reece, T.B. (2018). Optimized induction of beta common receptor enhances the neuroprotective function of erythropoietin in spinal cord ischemic injury. J. Thorac. Cardiovasc. Surg. *155*, 2505–2516.

Yoon, D., and Watowich, S.S. (2003). Hematopoietic cell survival signals are elicited through non-tyrosine-containing sequences in the membrane-proximal region of the erythropoietin receptor (EPOR) by a Stat5-dependent pathway. Exp. Hematol. *31*, 1310–1316.

Zang, H., Sato, K., Nakajima, H., McKay, C., Ney, P.A., and Ihle, J.N. (2001). The distal region and receptor tyrosines of the Epo receptor are non-essential for in vivo erythropoiesis. EMBO J. *20*, 3156–3166.

ISCI, Volume *17*

Supplemental Information

Transmembrane Protein Aptamer Induces Cooperative Signaling by the EPO Receptor and the Cytokine Receptor β-Common Subunit

Li He, Emily B. Cohen, Anne P.B. Edwards, Juliana Xavier-Ferrucio, Katrine Bugge, Ross S. Federman, Devin Absher, Richard M. Myers, Birthe B. Kragelund, Diane S. Krause, and Daniel DiMaio

Figure S1.

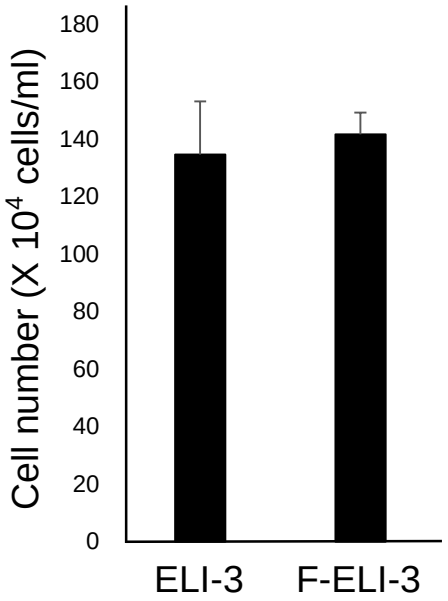
Cell number (X 10^4 cells/ml)
180
160
140
120
100
80
60
40
20
0
ELI-3
F-ELI-3

Figure S2.

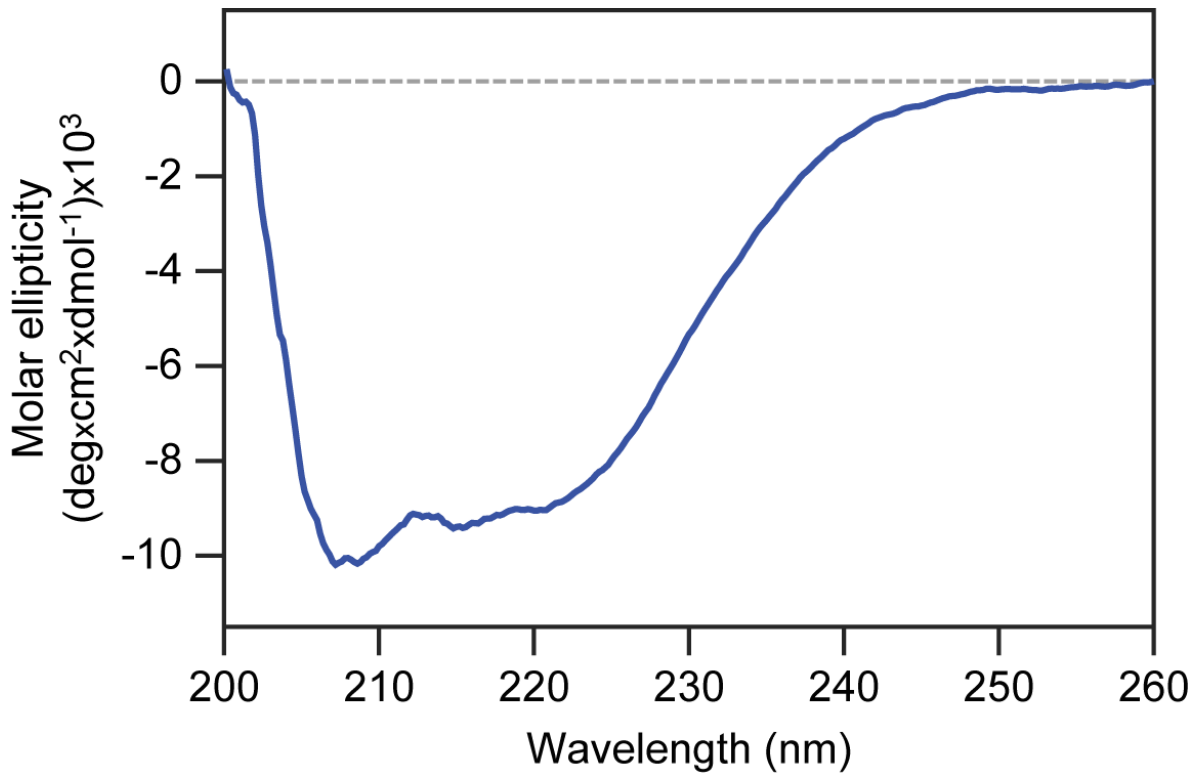
Molar ellipticity
(degxcm²xdmol⁻¹)x10³
0
-2
-4
-6
-8
-10
200
210
220
230
240
250
260
Wavelength (nm)

Figure S3.

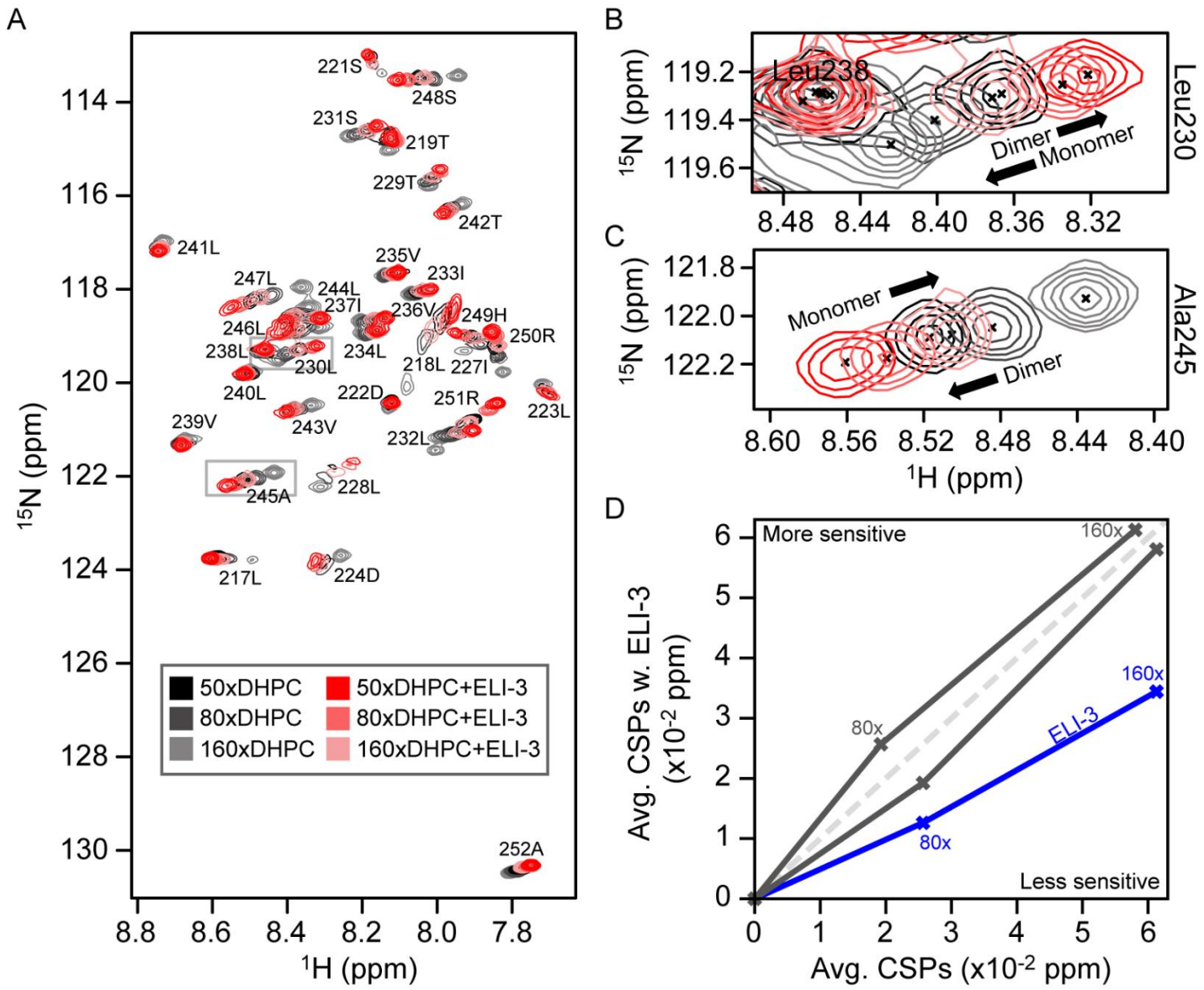
A
B
C
D
^{15}N (ppm)
^{1}H (ppm)
221S
248S
231S
219T
229T
242T
241L
235V
233I
247L
244L
237I
236V
249H
246L
250R
238L
230L
234L
218L
227I
240L
222D
251R
223L
239V
243V
232L
245A
228L
217L
224D
252A
50xDHPC
80xDHPC
160xDHPC
50xDHPC+ELI-3
80xDHPC+ELI-3
160xDHPC+ELI-3
Leu238
Dimer
Monomer
Leu230
Monomer
Dimer
Ala245
More sensitive
Less sensitive
160x
80x
ELI-3
Avg. CSPs w. ELI-3 (x10^{-2} ppm)
Avg. CSPs (x10^{-2} ppm)

Figure S4.

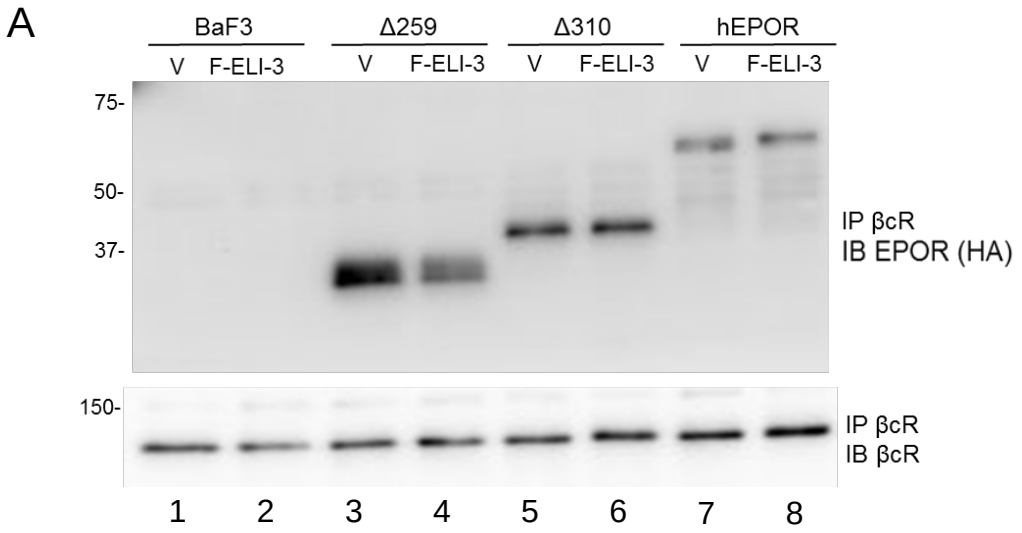
A
BaF3
Δ259
Δ310
hEPOR
V F-ELI-3 V F-ELI-3 V F-ELI-3 V F-ELI-3
75-
50-
37-
IP βcR
IB EPOR (HA)
150-
IP βcR
IB βcR
1 2 3 4 5 6 7 8

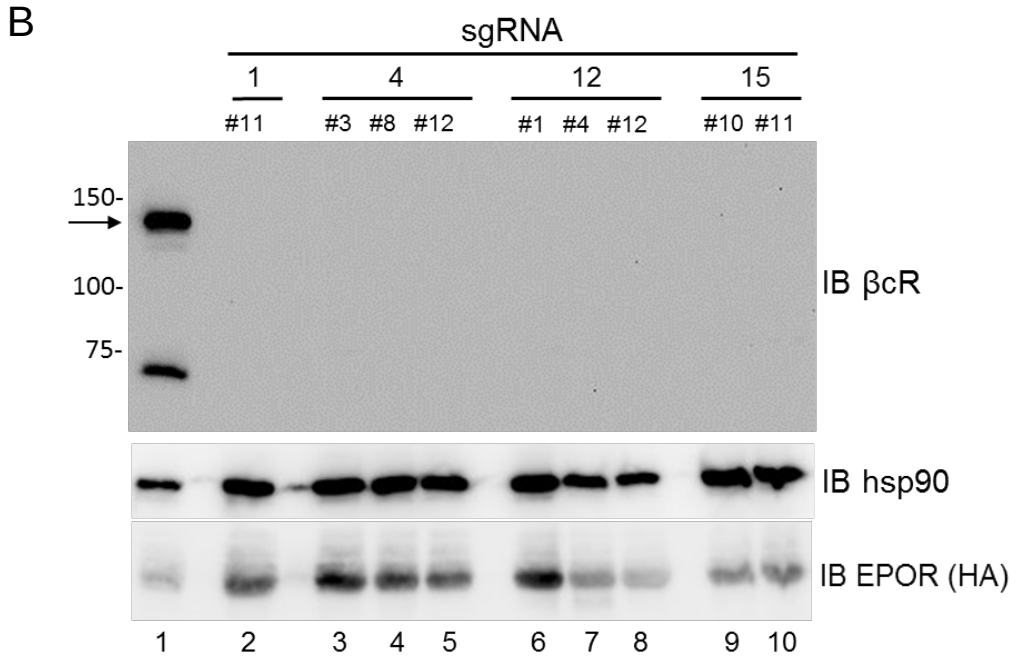
B
sgRNA
1
4
12
15
#11
#3 #8 #12
#1 #4 #12
#10 #11
150-
100-
75-
IB βcR
IB hsp90
IB EPOR (HA)
1 2 3 4 5 6 7 8 9 10

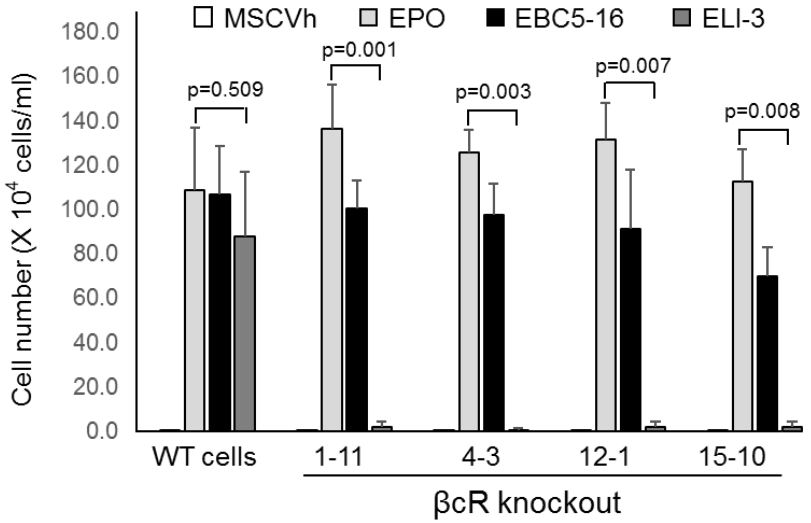
C
MSCVh
EPO
EBC5-16
ELI-3
Cell number (X 10^4 cells/ml)
180.0
160.0
140.0
120.0
100.0
80.0
60.0
40.0
20.0
0.0
p=0.509
p=0.001
p=0.003
p=0.007
p=0.008
WT cells
1-11
4-3
12-1
15-10
βcR knockout

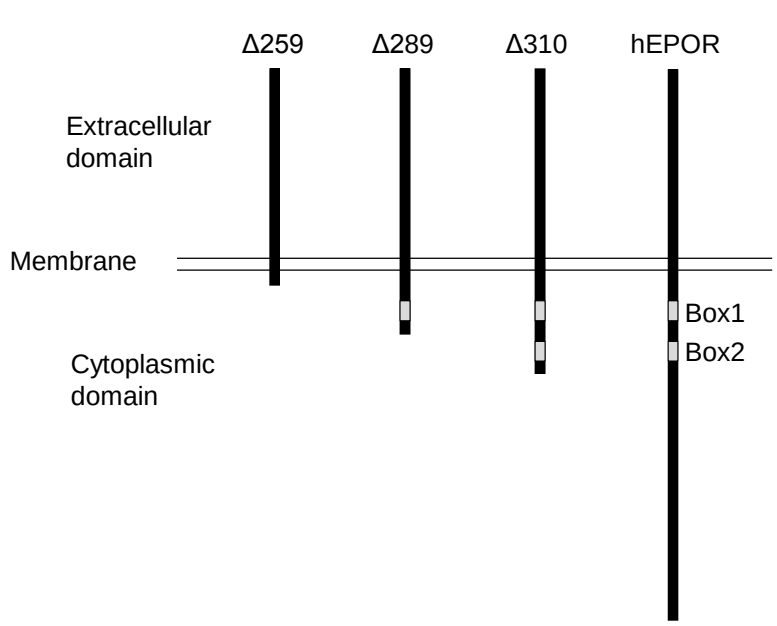
D
Δ259
Δ289
Δ310
hEPOR
Extracellular domain
Membrane
Cytoplasmic domain
Box1
Box2

Figure S5.

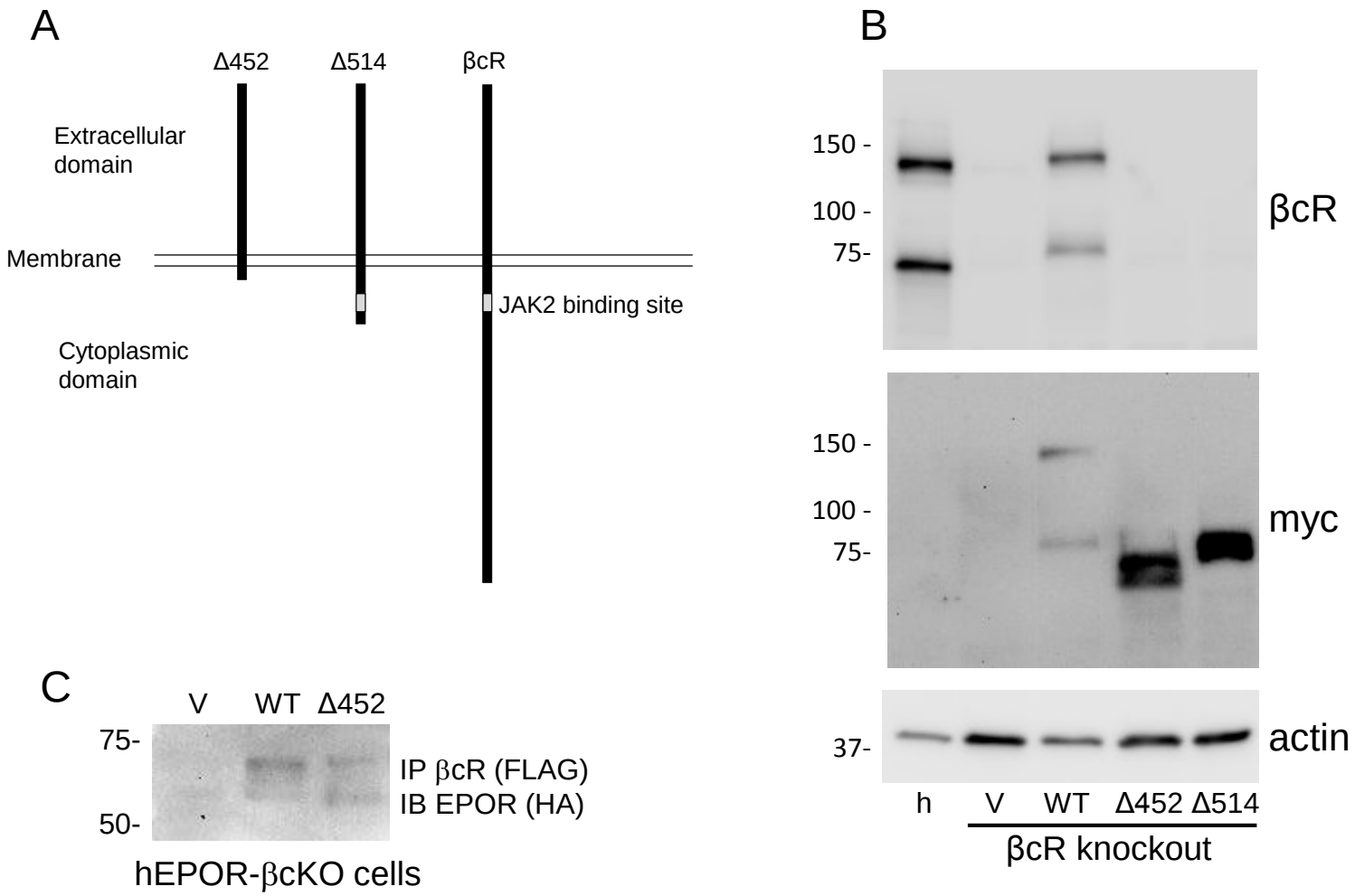
A
Δ452
Δ514
βcR
Extracellular domain
Membrane
JAK2 binding site
Cytoplasmic domain
B
150 -
100 -
75-
βcR
150 -
100 -
75-
myc
37-
actin
h
V
WT
Δ452
Δ514
βcR knockout
C
V
WT
Δ452
75-
50-
IP βcR (FLAG)
IB EPOR (HA)
hEPOR-βcKO cells

Figure S6.

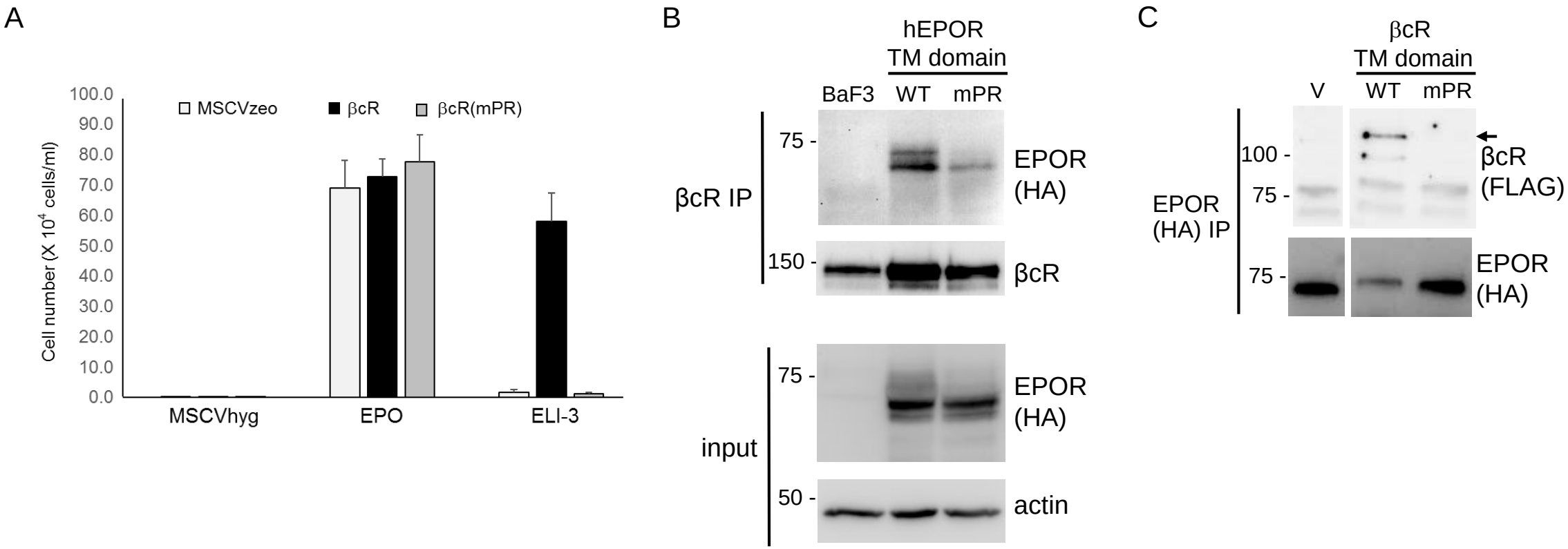
A
MSCVzeo
βcR
βcR(mPR)
Cell number (X 10^4 cells/ml)
100.0
90.0
80.0
70.0
60.0
50.0
40.0
30.0
20.0
10.0
0.0
MSCVhyg
EPO
ELI-3
B
hEPOR
TM domain
BaF3
WT
mPR
βcR IP
75 -
150 -
EPOR
(HA)
βcR
input
75 -
50 -
EPOR
(HA)
actin
C
βcR
TM domain
V
WT
mPR
EPOR
(HA) IP
100 -
75 -
75 -
βcR
(FLAG)
EPOR
(HA)

Figure S7.

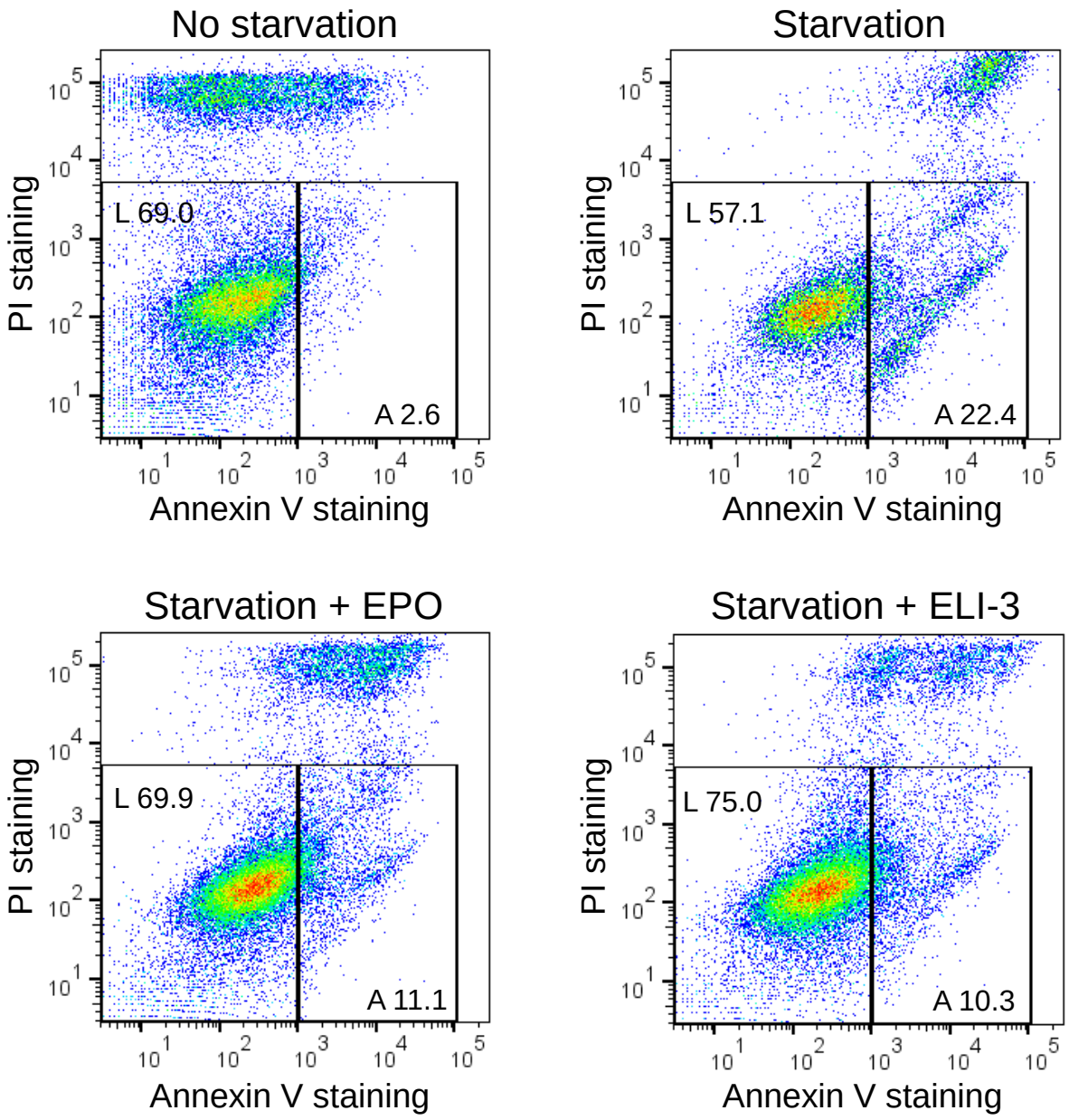
No starvation
PI staining
Annexin V staining
L 69.0
A 2.6
Starvation
PI staining
Annexin V staining
L 57.1
A 22.4
Starvation + EPO
PI staining
Annexin V staining
L 69.9
A 11.1
Starvation + ELI-3
PI staining
Annexin V staining
L 75.0
A 10.3

Supplemental Figure Legends

Figure S1. Activity of FLAG-tagged ELI-3, Related to Figure 2A. BaF3/hEPOR cells expressing ELI-3 or FLAG-tagged ELI-3 (F-ELI-3) were incubated in medium lacking IL-3. The number of live cells four days after IL-3 removal is shown. The averaged results and standard deviation of three independent experiments are shown.

Figure S2. ELI-3 forms an α-helix in detergent micelles, Related to Figure 2A. Far-UV circular dichroism (CD) spectrum of 8 µM ELI-3 in 80 times molar excess DHPC, 10 mM Na_2HPO_4/NaH_2PO_4 buffer (pH 7.2). Minima at 208 and 222 nm indicate significant α-helical structure.

Figure S3. ELI-3 shifts the EPOR transmembrane domain equilibrium towards the dimer state in DHPC micelles, Related to Figure 2A. **(A)** ^{1}H, ^{15}N- HSQC spectra of 220 µM ^{15}N-labeled $hEPOR_{217-252}$ +/- 285 µM ELI-3 in different DHPC ratios in accordance with the color key. **(B)** Zoom on Leu230 (grey box in **A**) and **(C**) Zoom on Ala245 (grey box in **A**). For both residues, addition of ELI-3 caused a shift towards the dimer state of EPOR-TMD (arrows) and decreased the sensitivity of the shift to the DHPC ratio. **(D**) Scatter plot of the average backbone amide chemical shift perturbations (CSPs) upon DHPC titration. In blue, average CSPs with (y-axis) or without (x-axis) molar excess ELI-3 added is plotted. In grey, the same x-values are plotted against an additional reference set without added ELI-3, which is mirrored along the diagonal. The substantial deviation of the blue data points from the diagonal suggests that addition of ELI-3 makes the dimer of EPOR-TMD less sensitive to dissociation upon dilution in DHPC micelles.

Figure S4. Identification and analysis of βcR knockout cells, Related to Figure 4. **(A)** Parental BaF3 cells or BaF3 cells expressing the wild-type hEPOR or the Δ259 or Δ310 hEPOR truncation mutant were infected with retroviruses to express MSCVp (V) or ELI-3. Cell extracts were immunoprecipitated with anti-βcR antibody and immunoblotted with the anti-HA antibody to detect EPOR in complex with βcR (top panel). The same membrane was stripped and reprobed with anti-βcR antibody (bottom panel). **(B)** Extracts prepared from BaF3/hEPOR cells (lane 1) or nine different clonal BaF3/h-βcKO cell lines generated with four different sgRNAs (1, 4, 12, 15) (lane 2 to lane 10) were immunoblotted with anti-βcR antibody (top panel). The same membrane was stripped and reprobed with anti-hsp90 antibody as a loading control (middle panel) and with anti-HA antibody to detect hEPOR (bottom panel). Arrow indicates band of expected size of full-length βcR. A band migrating with an apparent molecular mass of ~70 kDa may represent a different βcR isoform or a degradation product of βcR. **(C)** BaF3/hEPOR cells or the indicated clonal βcR knockout cells made in BaF3/hEPOR cell background were infected with MSCVhyg or MSCVhyg expressing EBC5-16 or ELI-3. After hygromycin selection, IL-3 was removed from the medium. Cells expressing MSCVhyg were incubated with medium containing EPO, as indicated. The number of live cells four days after IL-3 removal is shown. The averaged results and standard deviation of three independent experiments are shown. **(D)** Schematic diagram of the full-length hEPOR and the three hEPOR truncation mutants (Δ259, Δ289, and Δ310). The two JAK2 binding sites are shown in grey.

Figure S5. βcR truncation mutants and chimeras, Related to Figure 4. **(A)** Schematic diagram of full-length βcR and the two βcR truncation mutants (Δ452 and Δ514). JAK2 binding sites are shown in grey. **(B)** Myc/FLAG-tagged wild-type βcR and βcR truncation mutants were introduced into βcR knockout clone #15-10 by retroviral transduction and selection with Zeocin. Cell extracts were prepared, subjected to electrophoresis, and immunoblotted with anti-βcR (F12) antibody which recognizes only full-length βcR (top panel) or with anti-myc antibody (middle panel). Actin was used as loading control (bottom panel). **(C)** Extracts were prepared from BaF3/h-βcKO cells or these cells reconstituted with myc/FLAG-tagged wild-type βcR or βcR truncation mutant Δ452. Samples were immunoprecipitated with anti-FLAG to precipitate βcR and associated proteins. After gel electrophoresis and transfer, EPOR in the precipitate was detected by immunoblotting with anti-HA antibody.

Figure S6. Sequence elements required for complex formation between hEPOR and βcR, Related to Figure 7. **(A)** BaF3/h-βcKO cells expressing empty vector, wild-type βcR, or βcR containing the mPDGFβR TMD [βcR(mPR)] were infected with empty $MSCV_{hyg}$ vector or retrovirus expressing ELI-3 and selected with puromycin. Where indicated, $MSCV_{hyg}$ cells were also treated with EPO. The number of live

cells after 4 days in the absence of IL-3 is shown. **(B)** Top panels. Extracts were prepared from parental BaF3 cells and from BaF3 cells expressing hEPOR (WT) or hEPOR containing the murine PDGFβR TMD (mPR). Samples were immunoprecipitated by anti-βcR antibody to precipitate βcR and associated proteins. After gel electrophoresis and transfer, hEPOR associated with βcR was detected by immunoblotting with anti-HA. Bottom panels show input EPOR and actin as a loading control. **(C)** BaF3/h-βcKO cells were infected with empty vector (V) or reconstituted with myc/FLAG-tagged wild-type βcR (WT) or βcR chimera with the PDGFβR TMD (mPR). Samples were immunoprecipitated with anti-HA to precipitate hEPOR and associated proteins. After gel electrophoresis and transfer, βcR in the precipitate (arrow) was detected by immunoblotting with anti-FLAG antibody (top panel). Membrane was stripped and probed with anti-HA antibody to detect hEPOR.

Figure S7. Measurement of apoptosis by flow cytometry, Related to Figure 3B. P19 cells were treated as described in the legend to Figure 7B, bottom panel. Live and apoptotic cells are shown in boxed areas labeled L and A, respectively. The percentage of total cells in each box is shown. The panels show a set of representative flow cytometry 2D density plots.

TRANSPARENT METHODS

Vectors and Cloning

The HA-tagged hEPOR and HA-tagged mEPOR genes (originally obtained from S. Constantinescu, Ludwig Institute) were excised from the pBABE-puro retroviral vector and subcloned into pMSCV-neo (Clontech) using EcoRI and HpaI restriction sites. All positions in the hEPOR sequence are numbered according to the position in the mature, wild-type hEPOR. The Δ259, Δ289 and Δ310 hEPOR truncation mutants were constructed in pMSCV-neo by using Phusion High Fidelity DNA polymerase (New England Biolabs, #M0530L) to delete the DNA between codon 259, 289, and 310, respectively, and the stop codon. The F8 and F9 mutants of the hEPOR were constructed by replacing sequences encoding the cytoplasmic segment of the HA-hEPOR gene with a DNA gBlock™ Gene Fragment [Integrated DNA Technologies (IDT)] containing eight and nine tyrosine-to-phenylalanine mutations, respectively. The hEPOR chimera containing the mouse PDGFβ receptor TMD hEPOR(mPR) was described previously (Cammett et al., 2010). The myc/FLAG-tagged mouse βcR (*Csf2rb*) ORF clone was purchased from OriGene (cat. # MR226890L1) and subcloned into pMSCV-zeo vector (Addgene #75088) using BglII and EcoRI restriction sites (New England Biolabs). This clone contains a myc epitope followed by a DDK epitope (recognized by anti-FLAG antibody) at its C-terminus. Multiple silent mutations were introduced into this construct at sequences complementary to sgRNA15 to avoid recurring Cas9 nuclease activity (aaaacagccagtgtc to gaagcaaccggtctc). βcRΔ452 and Δ514 truncation mutants were constructed in myc/FLAG-tagged βcR lacking the sgRNA binding site by replacing sequences encoding the cytoplasmic domain of the βcR gene with DNA gBlock™ Gene Fragments (IDT) by using BstZ17I and EcoRI restriction sites. The βcR chimera containing the mouse PDGFβR TM domain [βcR(mPR)] was constructed similarly by using BamHI and BstZ17I restriction sites.

Cells and Retrovirus Infections

Human embryonic kidney (HEK) 293T cells were maintained in DMEM-10 medium: Dulbecco's Modified Eagle's Medium (DMEM) supplemented with 10% fetal bovine serum (FBS) (Gemini Bioproducts), 4 mM L-glutamine, 20 mM HEPES (pH 7.3), and 1X penicillin/streptomycin (P-S). To produce retrovirus stocks, 2 µg pantropic pVSV-G (Clontech), 3 µg pCL- (Imgenex), and 5 µg of the retroviral expression plasmid of interest were mixed with 250 µl of 2x HEBS. 250 µl 0.25 M calcium chloride was then bubbled into each mixture. The mixture (~500 µl) was incubated for 20 minutes at room temperature and then added drop-wise into 2.0 x 10^6 293T cells plated the day before in 100 mm tissue culture dishes in DMEM-10. The cells were incubated with the transfection mixture for 6-8 hours at 37°C, and the medium was replaced with 5 mL fresh DMEM-10 medium. The cells were incubated for another 48 hours at 37°C, then the viral supernatant was harvested, filtered through a 0.45 µm filter (Millipore), and either used immediately or stored at -80°C.

Murine interleukin-3 (IL-3)-dependent BaF3 and derivative cells were maintained in RPMI-10 media: RPMI-1640 supplemented with 10% heat-inactivated FBS, 5% WEHI-3B cell-conditioned medium (as the source of IL-3), 4 mM L-glutamine, 0.06 mM β-mercaptoethanol, and 1X P-S. BaF3 cells expressing HA-tagged hEPOR, HA-tagged mEPOR, and all EPOR mutants were generated by infecting BaF3 cells with pMSCV-neo vector containing the desired EPOR gene. 5x10^5 BaF3 cells were washed with phosphate buffered saline (PBS) and then re-suspended in 500 µl RPMI-10 medium with 4 µg/mL polybrene. 500 µl retroviral supernatant or 500 µl DMEM-10 for mock-infection was added to re-suspended cells and incubated for six hours at 37°C. After incubation, 9 ml RPMI-10 was added and the cells were incubated overnight at 37°C prior to selection in 1 mg/mL G418. Immunoblotting with anti-HA antibody confirmed the expression of full-length EPOR. Traptamers cloned in MSCV-puro were introduced into these cells by infection followed by selection in 1 µg/ml puromycin.

For growth factor independence assays, 2x10^5 BaF3 and derivative cells expressing the appropriate genes were washed in PBS three times to remove IL-3. Cell pellets were resuspended in 10 mL RPMI-10 IL-3-free medium, in which WEHI-3B cell-conditioned medium was not included. In control experiments, 0.6 U/ml human erythropoietin (Epoetin Alfa, Amgen) was added to the growth medium. Viable cells were counted four to six days after IL-3 removal. All IL-3 tests were performed in three independent biological replicates (*i.e.*, independent infections to express traptamers). All reported experiments included positive and negative controls that performed as expected, and no outliers in these experiments were excluded. All graphs show average values for IL-3 tests +/- SEM. Statistical significance of differences between control and experimental samples was evaluated by two-tailed Student's t-tests with unequal variance, performed using T.TEST function in Microsoft Excel (2013).

Retroviral Library Construction, Selection, and Deep Sequencing

To isolate new traptamers that activated the hEPOR, we used the YX4 traptamer expression library, which encodes short proteins with a 24-residue randomized hydrophobic segment expressed from the MSCVpuro

retroviral vector (Scheideman et al., 2012). Five wells of $5x10^5$ BaF3/hEPOR cells were plated in a 12-well plate in 500 µL of RPMI-IL-3. Five hundred microliters of 20X concentrated MSCVpuro-YX4 virus was added to each well. Polybrene was added to a final concentration of 4 µg/mL. Cells were incubated for four hours at 37°C and then transferred to individual 25 cm^2 flasks containing 9 mL of RPMI-IL-3 with polybrene. One day post-infection, 1 µg/mL puromycin was added to each flask. After puromycin selection, $5x10^5$ cells from each pool were washed once in PBS and resuspended in 10 mL RPMI-IL-3-free medium. After eight days of selection, $1x10^6$ cells from each pool were combined and harvested, and genomic DNA was isolated. PCR primers were designed to anneal to the common flanking sequence on each side of the randomized segment of the library (forward: 5'-CTACGACGTGCCCGACTAC-3'; reverse: 5'-GCAGACCTGTACAGGAGCATT-3'). These primers were used to amplify the starting plasmid library or genomic DNA from selected cells. Illumina sequencing adapters were then ligated to the ends of the pooled amplification products after they were digested and repaired. 2x72bp sequence reads were generated by Genome Analyzer IIx sequencing (Illumina). ~9 million and ~4.5 million quality filtered reads with the proper forward and reverse sequences were obtained from genomic and plasmid DNA, respectively. The forward and reverse reads were aligned, assembled into open reading frames, and translated. After excluding frameshift mutations, the remaining abundant protein sequences were grouped according to sequence similarity, and the number of sequences in each group was counted to assess selection of optimal traptamers. Codon-optimized versions of enriched traptamer sequences identified by deep sequencing were constructed by using double-stranded DNA gBlock™ Gene Fragments (IDT) and cloned into pMSCVpuro using BstXI and BamHI restriction sites.

Immunoprecipitation and Immunoblotting

Prior to harvest, BaF3 cells and their derivatives were grown in medium containing IL3- and then starved in RPMI-10 IL-3-free media for 3 hrs at 37°C. In some cases, cells were acutely stimulated with 5 U/mL EPO for 5 min at 37°C or with 5% WEHI-3B cell-conditioned medium (as the source of IL-3) for 15 min at 37°C. Cells were then washed twice with ice-cold PBS containing 1 mM phenylmethylsulfonyl fluoride (PMSF). For phosphotyrosine and phospho-protein blots, 1X HALT Protease and Phosphatase Inhibitor Cocktail (Thermo Scientific) and 500 µM hydrogen peroxide-activated sodium metavanadate were also added to the wash solution. Cells were lysed in FLAG-lysis buffer (50 mM Tris pH 7.4, 150 mM NaCl, 1 mM EDTA, 1% Triton-100) supplemented with protease and phosphatase inhibitors as described above. All lysates were incubated on ice for 20 minutes, followed by centrifugation at 14,000 rpm for 30 minutes at 4°C. The total protein concentration of the supernatants was determined using a bicinchoninic acid (BCA) protein assay kit (Pierce).

To immunoprecipitate HA-tagged EPORs for phosphotyrosine blotting, either 8 µl of a rabbit anti-EPOR polyclonal antibody (clone C-20, Santa Cruz Biotechnology) or 2 µl of anti-HA antibody (clone C29F4, Cell Signaling) was added to 0.4 mg of total protein and rotated overnight at 4°C. 50 µl Protein A Sepharose bead slurry was added and rotated for two hours at 4°C. To immunoprecipitate FLAG-tagged traptamers or myc/FLAG-tagged βcR, 50 µl of anti-FLAG M2 matrix gel (Sigma-Aldrich) was added to 0.5 mg of total protein and rotated overnight at 4°C. To immunoprecipitate βcR for phosphotyrosine blotting, 8 µl of a mouse anti-IL-3/IL-5/GM-CSFRβ antibody (Clone F-12, Santa Cruz Biotechnology) was added to 0.5 mg of total protein and rotated overnight at 4°C. 50 µl Protein A/G PLUS-Agarose bead slurry (Santa Cruz Biotechnology) was added and rotated for 2 h at 4°C. Immunoprecipitated samples were subjected to SDS-PAGE and immunoblotting.

Immunoprecipitated samples were washed four times with 1 mL NET-N buffer (100 mM NaCl, 0.1 mM EDTA, 20 mM Tris-HCl pH 8.0, 0.1% Nonidet P-40) supplemented with protease and phosphatase inhibitors as above, pelleted and re-suspended in 2x Laemmli sample buffer (2x SB) with 200 mM dithiothreitol (DTT) and 5% β-mercaptoethanol (β-ME). Precipitated proteins and whole cell lysates were heated at 95°C for 5 min and then resolved by SDS-PAGE on either 7.5%, 10% or 20% polyacrylamide gels according to the size of the protein. The resolving gel was then transferred by electrophoresis to a 0.2 µm nitrocellulose membrane. SDS was added to the transfer buffer for membranes used to detect phosphorylated proteins.

Membranes were blocked with gentle agitation for two hours at room temperature in 5% nonfat dry milk/TBST (1X Tris buffered saline plus 0.1% Tween-20). Mouse anti-phosphotyrosine monoclonal antibody PY100 (Cell Signaling) was used to detect the phosphorylated EPOR and βcR. To detect the phosphorylated forms of signaling proteins, the following antibodies were used: anti-phospho-JAK2 (Tyr1008) (clone D4A8, Cell Signaling); anti-phospho-STAT5 (Y694) #9351 (Cell Signaling); anti-phospho-MEK1/2 (Ser217/221) #9121 (Cell Signaling); anti-phospho-p44/42 MAPK (Erk1/2) (Thr202/Tyr204) #9101 (Cell Signaling). An HRP-conjugated mouse anti-HA (clone 6E2, Cell Signaling) was used to detect the HA-tagged EPORs and all EPOR mutants. An IL-3/IL-5/GM-CSFRβ antibody (clone F-12) (Santa Cruz Biotechnology) was used to detect the βcR. To detect total JAK2, STAT5, MEK and ERK, the following antibodies were used: anti-JAK2

(clone D2E12, Cell Signaling); anti-STAT5 #9363 (Cell Signaling); anti-MEK1/2 #9122 (Cell Signaling); anti-p44/42 MAPK (Erk1/2) Antibody #9102 (Cell Signaling). All antibodies were used at 1:1000 dilution except for the IL-3/IL-5/GM-CSFRβ antibody (clone F-12), which was used at 1:200 dilution. Membranes were incubated overnight with gentle agitation in primary antibody at 4°C, washed five times in TBST, and then incubated with gentle agitation for one hour at room temperature in donkey anti-mouse or donkey anti-rabbit HRP (Jackson Immunoresearch), as appropriate, at a 1:10,000 dilution. To re-probe, membranes were stripped in Restore Western Stripping Buffer (Thermo Scientific) for 15 min at room temperature with gentle agitation, washed five times in TBST, blocked in 5% milk/TBST for one hour at room temperature, and incubated overnight at 4°C with the corresponding antibody as described above. Membranes were incubated with Super Signal West Pico or Femto Chemiluminescent Substrates (Pierce) to detect protein bands.

Expression and Purification of Peptides for Circular Dichroism and NMR Spectrometry

FLAG-tagged ELI-3 was cloned into the pGEX-4T1 vector with an additional TEV cleavage site in the order: GST-thrombin cleavage site-TEV cleavage site- FLAG-tag-transmembrane sequence as described (He et al., 2017). DNA encoding $hEPOR_{217-252}$ was previously described (Bugge et al., 2015). Plasmids were transformed into *E. coli* BL21(DE3), and the cells grown in either unlabeled LB medium or in ^{15}N-labelled M9 medium supplemented with ampicillin to a cell density of 0.8 at OD_{600}. Protein expression was induced at 37ºC with 1 mM isopropyl β-D-1-thiogalactopyranoside (IPTG), and cells were harvested 4 hours after induction. $hEPOR_{217-252}$ and the ELI-3 fusion-proteins were expressed in inclusion bodies, which were harvested by three cycles of sonication and centrifugation. Inclusion bodies were washed in 50 mM Tris-HCl, pH 7.4 and solubilized in 1.5% (w/v) N-lauroylsarcosine and 100 mM dithiothreitol (DTT) in 50 mM Tris-HCl, pH 7.4. After gentle agitation overnight, the insoluble material was removed by centrifugation at 12,000 x g and the solubilized proteins dialyzed two times against four L of 0.5% (w/v) N-lauroylsarcosine in 50 mM Tris-HCl, pH 7.4. GST was cleaved off with thrombin (3 units/mL), and the released peptides were purified utilizing a chloroform/methanol extraction as described (Bugge et al., 2015), dried under a continuous flow of N_2 gas, and stored at -20˚C until use.

Circular Dichroism Spectrometry

A far-UV CD spectrum was recorded on 8 µM ELI-3 in 80 times molar excess of 1,2-dihexanoyl-sn-glycero-3-phosphocholine (DHPC) (0.6 mM), 10 mM Na_2HPO_4/NaH_2PO_4 buffer (pH 7.2) at 37°C using 10 nm/min scan speed, a bandwidth of 1 nm and 2 s response using a Jasco J-810 spectropolarimeter and a path length of 0.1 cm. 15 scans were accumulated, averaged, background corrected and smoothened. The background spectrum was recorded with identical settings on 0.6 mM DHPC in 10 mM Na_2HPO_4/NaH_2PO_4 buffer (pH 7.3) at 37°C.

Nuclear Magnetic Resonance Spectrometry

All $^{1}H,^{15}N$-HSQC NMR spectra were recorded at 37˚C on a 750 MHz (^{1}H) AVANCE III Bruker spectrometer equipped with a cryogenic probe using non-uniform sampling (Orekhov and Jaravine, 2011). Free induction decays were processed using the qMDD software (Orekhov and Jaravine, 2011) or Topspin (Bruker Biospin) and analysed using CcpNmr Analysis software (Vranken et al., 2005). Proton chemical shifts were referenced internally to 4,4-dimethyl-4-silapentane-1-sulfonic acid (DSS) at 0.00 ppm, with heteronuclei referenced by relative gyromagnetic ratios.

The concentration of $hEPOR_{217-252}$ was determined based on comparing the NMR peak volumes of the backbone amide peak of Asp222 in the $^{1}H,^{15}N$-HSQC spectra of ^{15}N-$hEPOR_{217-252}$ and ^{15}N-$hEPOR_{217-277}$ recorded with the same number of transients. The concentration of ^{15}N-$hEPOR_{217-277}$ was determined by absorption at 280 nm.

NMR spectra were recorded in 50 mM NaCl, 20 mM Na_2HPO_4/NaH_2PO_4 buffer (pH 7.3), 2 mM tris (2-carboxyethyl)phosphine (TCEP), 10% D_2O (v/v), 1 mM DSS and assignments of isolated peaks transferred from previous work on EPOR-TMD (He et al., 2017). Two identical ^{15}N-$hEPOR_{217-252}$ NMR samples were prepared by splitting a single stock solution (150 nmol ^{15}N-$hEPOR_{217-252}$ and 7.5 µmol DHPC) in two. 100 nmol ELI-3 in 5 µmol DHPC was added to one of these samples, and the same volume of buffer was added to the other sample. This way, all component concentrations of the two NMR samples were kept identical, except for ELI-3 and DHPC, for which the ratio (50 times excess) to protein was kept constant. Subsequently, a titration series for each of the two samples were obtained by adding DHPC to a ratio of 80- and 160-times molar excess.

Binding-induced weighted chemical shift perturbations (CSPs) were calculated as the weighted Euclidean distance between the peaks using $|\gamma N|/|\gamma H| = 0.154$. For each of the titration series (+/- ELI-3), the weighted CSPs were calculated relative to the shifts from the 50 times molar excess DHPC samples and averaged.

Construction and Analysis of Inducible Cell Lines

BaF3 cells were transduced to express an engineered version of the tetracycline-controlled transactivator protein, tTA-Advance, through retroviral infection with the pRetroX-Tet-Off Advanced (Clontech) vector and selection with G418. ELI-3 cloned in the expression vector pRetroX-TIGHT-puro (Clontech) was introduced into cells expressing tTA by retroviral infection and selection with puromycin. HA-hEPOR was retrovirally transduced with pMSCVneo (Clontech) and selected with EPO in the absence of IL-3.

$1x10^6$ BaF3/hEPOR/tTA/ELI-3 cells were seeded in 10 ml cultures in RPMI-10/IL-3 in the absence of doxycycline (DOX) or with 20, 40, 80, or 160 pg/ml DOX for 48 hours. Cells were washed twice with PBS and resuspended in RPMI-10 lacking IL-3 but with the same DOX concentrations for 3.5 hours. Cells were pelleted on ice in the presence of 15 ml Halt Phosphatase inhibitor (ThermoFisher) and 75 ml sodium metavanadate for 10 min at 1,500 rpm at 4°C. Cell extracts were prepared and electrophoresed as described using 20-30 µg of total protein. After transfer to 0.2 micron nitrocellulose membranes and blocking in 5% milk in TBST, blots were incubated overnight 4°C with 1:1000 Anti-PhosphoStat5 (Cell Signaling Technology 9351S) in 5% Milk in TBST. Blots were washed, incubated with 1:8000 secondary antibody, washed again and visualized using enhanced chemiluminescence. Blots were then stripped with stripping buffer (ThermoFisher), blocked, and re-probed with 1:1000 Anti-Total Stat5 (Cell Signaling Technology 94205).

Inhibitor Assays

To determine the effects of JAK2 and STAT5 chemical inhibitors on cell proliferation, $2x10^5$ cells were washed twice and re-suspended in RPMI-10 IL-3-free media. JAK Inhibitor IV (Calbiochem) was used to inhibit JAK2-induced signaling, and SH-4-54 (SelleckChem) was used to inhibit STAT5-induced signaling. Both inhibitors were dissolved in DMSO. DMSO only was used as a negative control. Viable cells were counted on day 4.

To determine the phosphorylation states of JAK2, STAT5, MEK, or ERK in cells treated with chemical inhibitors, cells were first starved in RPMI-10 IL-3-free media overnight. Then the chemical inhibitors were added for 30 min at 37°C before harvesting. In some cases, cells were acutely stimulated with 5 U/mL EPO for 5 min at 37°C.

Construction of βcR Knockout Cells and Rescue Experiments

The CRISPR-Cas9-based knock-out was conducted following the protocol described by Ran, *et al.* (Ran et al., 2013, Cao et al., 2016, Shalem et al., 2014). Four sgRNAs were designed using the online tool: http://crispr.mit.edu/. Their sequences are as follows: sgRNA1: AAGCCCATCTCTAACTACGATGG; sgRNA4: GGTCCAGTACAAGAAGAAATCGG; sgRNA12: GTGATGGAAAATCGTGTATAGGG; sgRNA15: GACACTGGCTGTTTTCTGTTAGG. Each sgRNA was cloned into the lentiCRISPRv2 plasmid (Addgene, #52961) using FastDigest Esp3I (Thermo Scientific). The plasmids were co-transfected into 293T cells with pMD.2G (Addgene, #12259) and psPAX2 (Addgene, #12260) to generate lentivirus stocks. After infection of BaF3 cells and puromycin selection, single cells were sorted into 96-well plates using BD FACS Aria II and cultured for 7-10 days. EPO was supplied in the medium to support cell growth in case knocking-out βcR impaired IL-3-dependent proliferation. Cell lines expanded from single cells were then tested individually by western blotting and sequencing to confirm knock-out. Because the sgRNA lentivirus encodes puromycin resistance, ELI-3 and EBC5-16 were expressed from MSCVhyg, which encodes hygromycin resistance. To express the βcR exogenously, myc/FLAG-tagged wild-type, truncated, and chimeric βcR constructs were packaged into retroviral vectors and then used to infect BaF3 cells expressing hEPOR but knocked out for βcR (clone #15-10). Infected cells were selected in 150 ng/ml zeocin. Expression of exogenous βcR was confirmed by immunoblotting with anti-myc antibody.

Erythroid Differentiation

To evaluate the erythropoietic and megakaryotic potential of cells expressing ELI-3, we performed the dual Mk/E colony assay as previously described (Sanada et al., 2016). Human granulocyte colony-stimulating factor (G-CSF) mobilized human peripheral blood enriched for CD34 staining (CliniMACS; Miltenyi) was stained with Lineage cocktail-BV510 (BD), CD34-BUV421 (Biolegend), CD38-PECF594 (BD), CD45Ra-BUV711, CD135-PE (Biolegend), CD36-PerCPCy5.5 (BD), CD110-APC (BD) and CD41a-APCH7 (BD) antibodies. Megakaryocyte erythroid progenitors (MEP: $Lin^-CD34^+CD45Ra^-CD135^-CD38^{mid}CD110^+CD36^-CD41a^-$), were sorted on a FACSAria, as previously described (Sanada et al., 2016).

Sorted MEPs were cultured in expansion media (100 ng/mL hFLT3, 100 ng/mL SCF, 20 ng/mL IL-3, 20 ng/mL IL-6, and 20 ng/mL hTPO, all from ConnStem) in StemSpan Serum Free Expansion Medium (Stem Cell Technologies) for 16 hours and transduced with retrovirus at MOI of 9. Briefly, 500 transduced cells were plated in two plates (250 cells/plate) of MegaCult C Medium plus Lipids (Stem Cell Technologies) with

0.5 µg/mL of puromycin (Sigma Aldrich), 10 ng/mL recombinant human interleukin 3 (rhIL-3), 10 ng/mL recombinant human interleukin 6 (rhIL-6), 25 ng/mL rhSCF (recombinant human stem cell factor), and 50 ng/mL rhTPO (recombinant human thrombopoietin) in the presence or absence of 3.0 U/mL recombinant human erythropoietin (rhEPO). All cytokines were from ConnStem except rhEPO (Amgen). After 12-14 days, the colonies were stained overnight with CD41-PE (Biolegend) and GpA-APC (BD) (1:100 dilution) and assessed by fluorescence microscopy (DMI6000B, Leica). Colonies were scored based on GpA and CD41a staining as megakaryocyte only (CFU-Mk), erythroid only burst forming unit (BFU-E), or megakaryocyte/erythroid (CFU-Mk/E), as previously described (Xavier-Ferrucio et al., 2018).

Tissue Protection Assays

P19 cells purchased from ATCC (CRL-1825) were maintained in AMEM 7.5/2.5 medium: Alpha Minimal Essential Medium (AMEM) supplemented with 7.5% bovine calf serum and 2.5% FBS. 12 h before infection, cells were plated at 10^4 cells/cm^2 in T-25 flasks. Cells were then infected with retroviruses expressing empty vector (MSCVp), FLAG-tagged EBC5-16, or FLAG-tagged ELI-3 and selected with 1µg/ml puromycin for 48 h. For starvation tests, cells were dissociated with trypsin, washed in starvation medium (AMEM supplemented with 5 µg/ml recombinant human insulin, 100 µg/ml human transferrin, 20 nM progesterone, 100 µM putrescine and 30 nM sodium selenite (all from Sigma-Aldrich)). For microscopic examination, cells were plated at 10^4 cells/cm^2 in 24-well plates with poly-lysine coated coverslips. In some cases, 2 U/ml rhEPO was added both 24 h before the starvation and concomitant with the starvation test. After 24 h, wells were subjected to cytospin centrifugation at 600 rpm for 10 min to capture non-adherent cells. After staining with 0.0002% 4′,6-diamidino-2-phenylindole (DAPI) (Fluoroshield Mounting Medium (Abcam)), nuclear fragmentation was determined using a fluorescent microscope (Zeiss Axio Imager), as previously described (Siren et al., 2001, Galli and Fratelli, 1993). 300-600 cells were counted for each sample.

For flow cytometry, P19 cells were plated at 10^4 cells/cm^2 in T-25 flasks in starvation medium or AMEM-7.5/2.5 medium. In some cases, 2 U/ml rhEPO was added both 24 hrs before and concomitant with the starvation. In some experiments, 10 µM JAK2 inhibitor IV was added during the period of starvation. After 22 hrs, cells were detached with trypsin and incubated in AMEM-7.5/2.5 medium at 37°C incubator for at least 30 min to allow membrane integrity to recover. Cells were then washed in cold PBS and stained with FITC-conjugated annexin V and propidium iodide (PI) using Dead Cell Apoptosis Kit (ThermoFisher, CAT# V13242) according to manufacturer's protocol. Stained cells were analyzed by BD FACS Aria II using green and red laser and were categorized into three groups: dead cells with high PI signal; live cells with low PI and low annexin V signal (L); apoptotic cells with low PI, high annexin V signal (A) (Fig. S5). The proportion of apoptotic cells was calculated as the A cell fraction divided by the A + L fraction.

Supplemental References

BUGGE, K., STEINOCHER, H., BROOKS, A. J., LINDORFF-LARSEN, K. & KRAGELUND, B. B. 2015. Exploiting hydrophobicity for efficient production of transmembrane helices for structure determination by NMR spectroscopy. *Anal Chem,* 87**,** 9126-31.

CAMMETT, T. J., JUN, S. J., COHEN, E. B., BARRERA, F. N., ENGELMAN, D. M. & DIMAIO, D. 2010. Construction and genetic selection of small transmembrane proteins that activate the human erythropoietin receptor. *Proc Natl Acad Sci USA,* 107**,** 3447-52.

CAO, J., WU, L., ZHANG, S. M., LU, M., CHEUNG, W. K., CAI, W., GALE, M., XU, Q. & YAN, Q. 2016. An easy and efficient inducible CRISPR/Cas9 platform with improved specificity for multiple gene targeting. *Nucleic Acids Res,* 44**,** e149.

GALLI, G. & FRATELLI, M. 1993. Activation of apoptosis by serum deprivation in a teratocarcinoma cell line: inhibition by L-acetylcarnitine. *Exp Cell Res,* 204**,** 54-60.

HE, L., STEINOCHER, H., SHELAR, A., COHEN, E. B., HEIM, E. N., KRAGELUND, B. B., GRIGORYAN, G. & DIMAIO, D. 2017. Single methyl groups can act as toggle switches to specify transmembrane protein-protein interactions. *eLife,* 6:e27701.

OREKHOV, V. Y. & JARAVINE, V. A. 2011. Analysis of non-uniformly sampled spectra with multi-dimensional decomposition. *Prog Nucl Magn Reson Spectrosc,* 59**,** 271-92.

RAN, F. A., HSU, P. D., WRIGHT, J., AGARWALA, V., SCOTT, D. A. & ZHANG, F. 2013. Genome engineering using the CRISPR-Cas9 system. *Nat Protoc,* 8**,** 2281-2308.

SANADA, C., XAVIER-FERRUCIO, J., LU, Y. C., MIN, E., ZHANG, P. X., ZOU, S., KANG, E., ZHANG, M., ZERAFATI, G., GALLAGHER, P. G. & KRAUSE, D. S. 2016. Adult human megakaryocyte-erythroid progenitors are in the CD34+CD38mid fraction. *Blood,* 128**,** 923-33.

SCHEIDEMAN, E. H., MARLATT, S. A., XIE, Y., HU, Y., SUTTON, R. E. & DIMAIO, D. 2012. Transmembrane protein aptamers that inhibit CCR5 expression and HIV coreceptor function. *J Virol,* 86**,** 10281-92.

SHALEM, O., SANJANA, N. E., HARTENIAN, E., SHI, X., SCOTT, D. A., MIKKELSON, T., HECKL, D., EBERT, B. L., ROOT, D. E., DOENCH, J. G. & ZHANG, F. 2014. Genome-scale CRISPR-Cas9 knockout screening in human cells. *Science,* 343**,** 84-87.

SIREN, A. L., FRATELLI, M., BRINES, M., GOEMANS, C., CASAGRANDE, S., LEWCZUK, P., KEENAN, S., GLEITER, C., PASQUALI, C., CAPOBIANCO, A., MENNINI, T., HEUMANN, R., CERAMI, A., EHRENREICH, H. & GHEZZI, P. 2001. Erythropoietin prevents neuronal apoptosis after cerebral ischemia and metabolic stress. *Proc Natl Acad Sci USA,* 98**,** 4044-9.

VRANKEN, W. F., BOUCHER, W., STEVENS, T. J., FOGH, R. H., PAJON, A., LLINAS, M., ULRICH, E. L., MARKLEY, J. L., IONIDES, J. & LAUE, E. D. 2005. The CCPN data model for NMR spectroscopy: development of a software pipeline. *Proteins,* 59**,** 687-96.

XAVIER-FERRUCIO, J., RICON, L., VIEIRA, K., LONGHINI, A. L., LAZARINI, M., BIGARELLA, C. L., FRANCHI, G., JR., KRAUSE, D. S. & SAAD, S. T. O. 2018. Hematopoietic defects in response to reduced Arhgap21. *Stem Cell Res,* 26**,** 17-27.